# Statistical Wave Field Theory

Roland Badeau[a]

[a]LTCI, Télécom Paris, Institut Polytechnique de Paris, Palaiseau, 91120, France

**Abstract**

In this paper, we introduce the foundations of the Statistical Wave Field Theory. This theory establishes the statistical laws of waves propagating in a closed bounded volume, that are mathematically implied by the boundary-value problem of the wave equation. These laws are derived from the Sturm-Liouville theory and the mathematical theory of dynamical billiards. They hold after many reflections on the boundary surface, and at high frequency. This is the first statistical theory of reverberation which provides the closed-form expression of the power distribution and the correlations of the wave field jointly over time, frequency and space inside the bounded volume, in terms of the geometry and the specific admittance of its boundary surface. The Statistical Wave Field Theory may find applications in various science fields, including room acoustics, electromagnetic theory, and nuclear physics.

*Keywords:* Statistical physics, wave equation, Helmholtz equation, reverberation

**Contents**



*Email address:* roland.badeau@telecom-paris.fr (Roland Badeau)

## 1. Introduction

The statistical modeling of wave phenomena has raised a constant interest over the past century, especially in acoustics and optics.

In the field of room acoustics, it is well known that when waves propagate in a bounded three-dimensional (3D) space, after many reflections on the room boundaries, and at high frequency, their collective behavior becomes stochastic, a physical phenomenon that is called *late reverberation*. During the 20th century, several researchers aimed to characterize mathematically various statistical properties of reverberation, *e.g.* over time (Moorer, 1979), frequency (Schroeder, 1962), time-frequency (Polack, 1988) and space (Cook *et al.*, 1955). In particular, the reverberation time, which is defined as the time it takes for the sound pressure level to reduce by 60 dB, received special attention, first with the empirical law proposed by Wallace Clement Sabine at the end of the 19th century from early experiments, which holds in a diffuse acoustic field and highly reverberant rooms (Joyce, 1975), then with the modified formula established by Carl F. Eyring (1930), which holds when the absorption at the boundary is larger, and later with the reverberation theory of Jean-Dominique Polack (1992), based on the mathematical theory of dynamical billiards.

In the field of underwater acoustics, many works were intended to emulate some physical properties of the surfaces and of the medium, including volume heterogeneities, through the introduction of an empirical probability distribution of random "scatterers" in a virtually infinite medium (Middleton, 1967a,b; Ol'shevskii, 1978; Middleton, 1987; Ratilal and Makris, 2005; Abraham, 2019). In particular, a general statistical theory of reverberation was presented in (Middleton, 1967a,b), with many key elements associated with the physical properties of the environment, as well as the parameters of the sensor system. Propagation and scattering in waveguides with randomly rough boundaries and random volume heterogeneities have also been addressed (Colosi, 2016; Ishimaru, 1978a,b). In particular, Ishimaru (1978a,b) also mentioned possible applications to atmospheric and biological media.

In the field of optics and optoelectronics, a broad coverage of the topic of fluctuations associated with random scattered waves can be found (Jakeman and Ridley, 2006; Goodman, 2000). Finally, irregular boundaries were explicitly modeled in (Ogilvy, 1991), which describes various classes of random surfaces and associated scattered fields, and cites many possible applications including medical ultrasonics, radar imaging, sonar detection, solid-state physics, optics, astronomy, and ultrasonic non-destructive testing.

Contrary to most of the previously-mentioned works from the underwater acoustics and optics literature dedicated to the statistical modeling of random scattered waves, the Statistical Wave Field Theory introduced in this paper is *not* another heuristic model that would be intended to emulate some physical properties of the medium or the boundary surface, through the introduction of random scatterers.

Instead, this is the very first theory that establishes mathematically the statistical laws of the solutions to the wave equation in a closed bounded domain. These statistical laws are derived from the Sturm-Liouville theory (Pearson, 2001) and the mathematical theory of dynamical billiards (Polack, 1992). They are actually deterministic and chaotic, but the Statistical Wave Field Theory translates them into the more accessible language of the theory of probability by modeling the source position as random. In addition, contrary to the previously-mentioned works, this theory explicitly and accurately accounts for the shape of the boundary, as complex as it may be, as well as the specific admittance of its surface.

Of course, the basic version of the theory presented in this paper achieves this difficult mathematical analysis in a much simpler setting than the one generally considered in underwater acoustics and in some other fields:

- The wave equation has to hold exactly in the whole domain. This means that the medium is lossless, homogeneous and at rest (Kuttruff, 2014, Chapter 1). So wave phenomena due to changes or fluctuations in the medium, such as refraction and dispersion, are not considered.

- The boundary surface has to be closed and bounded. In particular, no opening is allowed. Moreover, the shape of the boundary has to meet the mathematical conditions of a *mixing* dynamical billiard (Polack, 1992), a notion that is related to *diffusion*. Concretely, this means that most geometric shapes are allowed, especially those including irregular (rough) surfaces producing wave scattering. Indeed, even though there is no simple mathematical characterization of mixing billiards, there exist general results that show basically that the more the boundary is irregular, the more it is mixing, and on the contrary, the more it is smooth, the less it is mixing. In particular, the simplest possible geometric shape, namely the *sphere*, is excluded, because it is highly non-mixing. Nevertheless, there exist very smooth and simple geometric shapes such as the Bunimovich stadium (Bunimovich, 1979) which are mixing, though the mixing rate is rather slow in this case.

- The physical source is assumed punctual. Moreover, the receiver's response and directivity are not modeled; instead the Statistical Wave Field Theory describes the statistics of the wave field itself, as a function of space, time and frequency.

- All parameters of the problem, including the random source position and the boundaries of the domain, are assumed constant over time.

If we consider any physical problem where these assumptions hold, then no matter the exact shape of the boundary, no matter the regularity or irregularity of the surfaces, no matter the exact physical properties of the materials at the boundary: the solutions to the wave equation have to follow the laws of the Statistical Wave Field Theory, because these laws are mathematically implied by the boundary-value problem of the wave equation.

In room acoustics, these assumptions generally hold, so the Statistical Wave Field Theory is able to investigate the statistical properties of the room impulse response in a mixing room.

Let us now introduce the mathematical grounds of the Statistical Wave Field Theory. It is well known that the solutions to the wave equation in a bounded domain are characterized by the Helmholtz equation which, along with its boundary conditions, forms a particular Sturm-Liouville problem (Pearson, 2001). The Sturm-Liouville theory shows that this problem admits a discrete set of solutions, called *normal modes* (Kuttruff, 2014, Chapter 3). In several dimensions of space, the density of discrete modes increases with the frequency, in a way that has been investigated mathematically for the first time by Hermann Weyl (1911). Since then, a rich literature has been devoted to the study of asymptotic expansions of the modal density as a function of frequency $f$ when $f \to +\infty$, in various space dimensions and various boundary conditions (Arendt *et al.*, 2009). The case of a 3D space and of Robin's boundary condition, which is of special interest to us, was first addressed by the physicists Balian and Bloch (1970). Indeed, there is a strong connection between their asymptotic expansion of the modal density and the Statistical Wave Field Theory, which models the wave field as a random process. To put it simply, if there is no energy absorption at the boundary surface, then the wave field is asymptotically *wide sense stationary* (WSS): all normal modes are uncorrelated and carry the same quantity of power, so that the modal density as a function of frequency is proportional to the *power spectrum* of the wave field. If on the contrary there is energy absorption, then the wave field is non-stationary, and the Statistical Wave Field Theory proves that its statistics are actually related to the analytic continuation of the modal density to the domain of complex frequencies. In this paper, we will investigate the first and second order statistics of the wave field which result from the asymptotic expansion up to order 1 in frequency. Indeed, up to this order, wave propagation can be approximated by considering the trajectory of rays undergoing successive specular reflections on the boundary surface, which explains the relationship with the mathematical theory of dynamical billiards. So the Statistical Wave Field Theory is based on a high frequency approximation, in exactly the same way as geometric acoustics and optics. Consequently, wave-related phenomena such as edge diffraction are not taken into account in this paper (but they will be in future publications, through the second-order terms of the asymptotic expansion).

To sum up, the predictions of the Statistical Wave Field Theory hold in a particular region of the time-frequency plane that we depicted in a previous work (Badeau, 2019, Figure 1): in the frequency domain, at high frequency, so that the conditions of geometric acoustics and optics are met, and in the time domain, after the *mixing time* as defined by Polack (1992), so that the mixing conditions of a dynamical billiard are met. In this particular time-frequency region, both the reflections over time and the normal modes over frequency are dense enough to be represented with a smooth density function.

In room acoustics, the Statistical Wave Field Theory is the very first mathematical approach of reverberation that is able to express in closed-form the asymptotic statistics of the wave field as an explicit function of the boundary's shape, as complex as it may be, and of the specific admittance of the boundary surfaces, which characterizes completely the physical properties of these surfaces regarding wave reflection. In particular, it permits us to retrieve the previously-mentioned statistical properties of reverberation, including (Cook *et al.*, 1955; Schroeder, 1962; Moorer, 1979; Polack, 1988). It is also the very first approach of reverberation which is able to express in closed-form, not only the reverberation time as a function of frequency, as in Sabine's and Eyring's formulas (Eyring, 1930), but also the exact asymptotic distribution of the sound power as a function of *space* and frequency inside the room's volume. Moreover, it can do it not only in mixing rooms, where the reverberation time is uniform and isotropic, but also in certain non-mixing rooms, where the reverberation time is a function of both the angle and the frequency (the latter case will be addressed in a future publication).

In addition, due to its connection with (Balian and Bloch, 1970), we believe that this theory may also find applications in very different domains such as nuclear physics, *e.g.* to model the self-consistent field of a heavy nucleus, and electromagnetic theory, *e.g.* to model electromagnetic vector waves in a cavity with perfectly conducting boundary surfaces (sample applications of electromagnetic reverberation chambers are described in (Besnier and Démoulin, 2011)).

This paper is structured as follows: in Section 2, we introduce some acronyms and mathematical notations that will be used in the rest of the paper. Then in Section 3 we summarize a few fundamental notions regarding wave propagation, that we need to develop the Statistical Wave Field Theory, and in Section 3.6, we review a few statistical properties of reverberation that have been known in room acoustics and that the theory will permit us to retrieve. In Section 4, we briefly present the Wigner time-frequency distribution that we will use to characterize the second-order properties of non-stationary processes, and we list the three mathematical assumptions on which the Statistical Wave Field Theory relies. Then in Section 5 we introduce the *special* theory dedicated to Neumann's boundary condition, and in Section 6 we introduce the *general* theory dedicated to Robin's boundary condition. The main results of the Statistical Wave Field Theory are summarized in Sections 5.4 and 6.6. In Section 7, we discuss some current limitations of the theory, and we show how they could be overcome in future work. Finally, in Section 8 we summarize the main contributions of this paper, and propose a few extensions of the theory.

## 2. Acronyms and mathematical notations

**Acronyms:**

**ACF** auto-covariance function

**PCF** pseudo-covariance function

**RIR** room impulse response

**WSS** wide sense stationary

**Mathematical notations:**

- $\triangleq$: equal by definition to
- $\mathbb{N}$: set of whole numbers
- $\mathbb{R}$, $\mathbb{C}$: sets of real and complex numbers, respectively
- $\imath = \sqrt{-1}$: imaginary unit
- $\mathbb{R}_+$: set of nonnegative real numbers

- $[a, b]$: closed interval, including $a, b \in \mathbb{R}$, or closed line segment in the complex plane, bounded by $a, b \in \mathbb{C}$
- $]a, b[$: open interval, excluding $a$ and $b \in \mathbb{R}$
- $A \backslash B$: relative complement (set difference) of set $B$ in set $A$
- $A^* = A \backslash \{0\}$: set $A$ minus 0
- $A \subseteq B$: $A$ is a subset of $B$, possibly equal to $B$
- $\mathring{V}$: interior of a subset $V$ of $\mathbb{R}^3$
- $\overline{V}$: closure of a subset $V$ of $\mathbb{R}^3$
- $\partial V = \overline{V} \backslash \mathring{V}$: boundary of a subset $V$ of $\mathbb{R}^3$
- $|V|$: Lebesgue measure (volume) of a subset $V$ of $\mathbb{R}^3$
- $\lambda = \frac{1}{|V|}$: mean density of sources over space
- $S(A)$: surface area of a 2-dimensional sub-manifold $A$ of $\mathbb{R}^3$
- $\boldsymbol{x}$ (bold font), $z$ (regular): vector and scalar, respectively
- $\boldsymbol{P}_T$: $3 \times 2$ orthonormal matrix whose range space is parallel to plane $T \subset \mathbb{R}^3$
- $\|.\|_2$: Euclidean/Hermitian norm of a vector or a function
- $\overline{z}$: complex conjugate of $z \in \mathbb{C}$
- $\mathrm{Re}(z)$ (resp. $\mathrm{Im}(z)$): real (resp. imaginary) part of a complex number $z \in \mathbb{C}$
- $\boldsymbol{x}^\top$: transpose of vector $\boldsymbol{x}$
- $\boldsymbol{x}^H$: conjugate transpose of vector $\boldsymbol{x}$
- $A^\perp$: orthogonal complement of set $A$
- $\mathcal{S}(0, k)$: sphere centered at the origin and of radius $k$: $\mathcal{S}(0, k) = \{\boldsymbol{k} \in \mathbb{R}^3; \|\boldsymbol{k}\|_2 = k\}$
- $\mathcal{B}(\boldsymbol{s}, \varepsilon)$: open ball centered at $\boldsymbol{s} \in \mathbb{R}^3$ and of radius $\varepsilon$: $\mathcal{B}(\boldsymbol{s}, \varepsilon) = \{\boldsymbol{x} \in \mathbb{R}^3; \|\boldsymbol{x} - \boldsymbol{s}\|_2 < \varepsilon\}$
- $L^2(V)$ where $V$ is a Borel subset of $\mathbb{R}^3$: Hilbert space of measurable functions $f$ supported in $V$, such that $\|f\|_2 = \sqrt{\int_V |f(\boldsymbol{x})|^2 d\boldsymbol{x}} < +\infty$
- $\mathcal{S}(\mathbb{R}^n)$: Schwartz space of smooth functions on $\mathbb{R}^n$, whose derivatives of all orders are rapidly decreasing
- $\langle T | \psi \rangle$: value of the tempered distribution $T$ on the test function $\psi \in \mathcal{S}(\mathbb{R}^n)$

- $\delta$: Dirac delta function
- $\delta_{n_1,n_2}$: Kronecker delta: $\delta_{n_1,n_2} = 1$ if $n_1 = n_2$, $\delta_{n_1,n_2} = 0$ otherwise
- $H(t)$: Heaviside function: $H(t) = 1\ \forall t > 0$ and $H(t) = 0\ \forall t < 0$
- $\text{sign}(t)$: sign function: $\text{sign}(t) = 1\ \forall t > 0$ and $\text{sign}(t) = -1\ \forall t < 0$
- $\text{sinc}(x) = \frac{\sin(x)}{x}$: cardinal sine function
- $\Delta\phi(\boldsymbol{x})$: Laplacian of function $\phi(\boldsymbol{x})$
- Convolution of two functions $\psi_1$ and $\psi_2 : \mathbb{R} \to \mathbb{C}$:

$$(\psi_1 * \psi_2)(t) = \int_{\tau\in\mathbb{R}} \psi_1(\tau)\psi_2(t-\tau)d\tau$$

- 1D direct and inverse Fourier transforms of a function $\psi : \mathbb{R} \to \mathbb{C}$:

$$\widehat{\psi}(f) = \int_{t\in\mathbb{R}} \psi(t)e^{-2\imath\pi ft}dt \quad \text{and} \quad \psi(t) = \int_{f\in\mathbb{R}} \widehat{\psi}(f)e^{+2\imath\pi ft}df \tag{1}$$

- 3D direct and inverse Fourier transform of a function $\psi : \mathbb{R}^3 \to \mathbb{C}$:

$$\widehat{\psi}(\boldsymbol{k}) = \int_{\boldsymbol{x}\in\mathbb{R}^3} \psi(\boldsymbol{x})e^{-2\imath\pi\boldsymbol{k}^\top\boldsymbol{x}}d\boldsymbol{x} \quad \text{and} \quad \psi(\boldsymbol{x}) = \int_{\boldsymbol{k}\in\mathbb{R}^3} \widehat{\psi}(\boldsymbol{k})e^{+2\imath\pi\boldsymbol{k}^\top\boldsymbol{x}}d\boldsymbol{k} \tag{2}$$

- $\mathbb{E}[X]$: expected value of a random variable $X$
- Covariance of two complex random variables $X$ and $Y$:

$$\text{cov}[X,Y] = \mathbb{E}[(X - \mathbb{E}[X])\overline{(Y - \mathbb{E}[Y])}]$$

## 3. Fundamentals of waves revisited

In this section, we summarize a few fundamental notions regarding wave propagation, that we need to develop the Statistical Wave Field Theory in the remaining sections of this paper. Most of these notions are well-known and are described for instance in (Morse and Ingard, 1968). However, a few concepts presented here are not standard, such as the *B-function* that will be introduced in Section 3.2, and the *source response* that we will introduce now, as well as its closed-form expressions given in Sections 3.3.2 and 3.4.2. Moreover, we will also introduce here a few non-standard notations.

In a simply connected domain $V \subseteq \mathbb{R}^3$, the homogeneous wave equation states that

$$\Delta p(\boldsymbol{x},t) - \frac{1}{c^2}\frac{\partial^2 p(\boldsymbol{x},t)}{\partial t^2} = 0 \tag{3}$$

where $p(\boldsymbol{x},t)$ is the wave amplitude at position $\boldsymbol{x} \in \mathring{V}$ and time $t \in \mathbb{R}$, $\Delta$ is the Laplacian, and $c$ is the propagation speed of the wave. This differential equation governs the propagation of sound waves in any lossless fluid (so it ignores the possible attenuation of sound in the medium) and is therefore of central importance for almost all acoustical phenomena. It holds not only for the sound pressure $p$, but also for the density and temperature variations. Moreover, it relies on the assumption that the medium is homogeneous and at rest, which guarantees that the speed of sound $c$ is constant with respect to space and time (Kuttruff, 2014, Chapter 1). In nuclear physics, $p$ might be the single particle wave function in the independent particle approximation. Then (3) with a suitable boundary condition is an idealization of the actual self-consistent field of a heavy nucleus (Balian and Bloch, 1970). Finally, in electromagnetic theory, equation (3) governs electromagnetic vector waves in a cavity with perfectly conducting boundary surfaces (Balian and Bloch, 1971).

By applying the one-dimensional (1D) Fourier transform (1) w.r.t. time to equation (3), we get the Helmholtz equation[1]:

$$\Delta\phi(\boldsymbol{x}) + 4\pi^2 k^2 \phi(\boldsymbol{x}) = 0 \tag{4}$$

where the scalar $k = \frac{f}{c}$ is the *wave number*[2] and $f$ denotes the frequency.

Given a punctual source position $\boldsymbol{x}_0 \in \mathring{V}$ and a space position $\boldsymbol{x} \in \mathring{V}$, we define the *source response* $p$ as the unique causal solution to the following inhomogeneous wave equation: $\forall t \in \mathbb{R}$,

$$\Delta p(\boldsymbol{x}, \boldsymbol{x}_0, t) - \frac{1}{c^2}\frac{\partial^2 p(\boldsymbol{x}, \boldsymbol{x}_0, t)}{\partial t^2} = -\delta(\boldsymbol{x} - \boldsymbol{x}_0)\dot{\delta}(t). \tag{5}$$

Note that the right member of equation (5) involves the derivative of a Dirac delta function over time, in order to account for the fact that the response of a physical source is always zero at the zero frequency (Morse and Ingard, 1968, Chapter 7). Replacing the derivative $\dot{\delta}(t)$ with $\delta(t)$ in (5) would lead to the usual definition of the *room impulse response* (RIR) $h(\boldsymbol{x}, \boldsymbol{x}_0, t)$ in room acoustics, which is the causal Green's function of the wave equation (3). The RIR $h$ is the unique causal primitive of the source response $p$ defined in (5).

In the free field (i.e. when $V = \mathbb{R}^3$), the source response $p$ is expressed as

$$p(\boldsymbol{x}, \boldsymbol{x}_0, t) = \frac{\dot{\delta}\left(t - \frac{\|\boldsymbol{x}-\boldsymbol{x}_0\|_2}{c}\right)}{4\pi\|\boldsymbol{x} - \boldsymbol{x}_0\|_2}. \tag{6}$$

### *3.1. Green's function*

For any simply connected domain $V \subseteq \mathbb{R}^3$, given a punctual source position $\boldsymbol{x}_0 \in \mathring{V}$ and a space position $\boldsymbol{x} \in \mathring{V}$, a Green's function $G$ of the Helmholtz equation (4) is a particular solution to the following inhomogeneous Helmholtz equation:

$$\Delta G(\boldsymbol{x}, \boldsymbol{x}_0, k) + 4\pi^2 k^2 G(\boldsymbol{x}, \boldsymbol{x}_0, k) = -\delta(\boldsymbol{x} - \boldsymbol{x}_0). \tag{7}$$

[1]In (4), $\phi$ denotes the 1D Fourier transform of $p$ w.r.t. time $t$, so it is implicitly a function of frequency $f$.

[2]Note the unusual presence of the term $4\pi^2$ in (4), which induces a normalization of the wave number different from what is usually found in the literature. This convention is related to our definition of the Fourier transform in (1) as a function of the *frequency*, instead of the *pulsation* or *angular frequency*.

The inverse 1D Fourier transform (1) of $G$ w.r.t. frequency $f = ck$,

$$g(\boldsymbol{x}, \boldsymbol{x}_0, t) = \int_{f \in \mathbb{R}} G(\boldsymbol{x}, \boldsymbol{x}_0, \tfrac{f}{c})\, e^{2\imath\pi f t} df, \tag{8}$$

is such that its time derivative $\dot{g}(\boldsymbol{x}, \boldsymbol{x}_0, t)$ is a solution to (5). However, depending on the choice of a particular solution $G$ to equation (7), the function $\dot{g}(\boldsymbol{x}, \boldsymbol{x}_0, t)$ may not be causal, so in general $\dot{g}(\boldsymbol{x}, \boldsymbol{x}_0, t)$ differs from the causal source response $p(\boldsymbol{x}, \boldsymbol{x}_0, t)$ by a function which is a solution to the homogeneous wave equation (3).

In the free field ($V = \mathbb{R}^3$), any Green's function $G$ solution to (7) can be written as the translation over space of some Green's function $G_0$ for a source located at $\boldsymbol{x}_0 = \mathbf{0}$:

$$G(\boldsymbol{x}, \boldsymbol{x}_0, k) = G_0(\boldsymbol{x} - \boldsymbol{x}_0, k). \tag{9}$$

In this paper, we will consider the real Green's function

$$G_0(\boldsymbol{x}, k) = \frac{\cos(2\pi k \|\boldsymbol{x}\|_2)}{4\pi \|\boldsymbol{x}\|_2}, \tag{10}$$

which is such that function $\dot{g}$ is an odd function of time. In the free field, the relationship between $\dot{g}$ and the source response $p$ in (6) can be expressed as

$$p(\boldsymbol{x}, \boldsymbol{x}_0, t) = 2H(t)\, \dot{g}(\boldsymbol{x}, \boldsymbol{x}_0, t) \tag{11}$$

where $H(t)$ denotes the Heaviside function, which is such that $H(t) = 1$ $\forall t > 0$ and $H(t) = 0$ $\forall t < 0$. The 3D Fourier transform (2) of $G_0(\boldsymbol{x}, k)$ w.r.t. space is

$$\widehat{G}_0(\boldsymbol{k}, k) = \frac{1}{4\pi^2(\|\boldsymbol{k}\|_2^2 - k^2)}. \tag{12}$$

Note that the real Green's function $G_0$ in (10) differs from the complex one that is usually found in the literature, $G_c(\boldsymbol{x}, k) = \frac{e^{-2\imath\pi k \|\boldsymbol{x}\|_2}}{4\pi \|\boldsymbol{x}\|_2}$, which satisfies the Sommerfeld radiation condition[3] (Schot, 1992). Actually, our choice of using the real Green's function $G_0$ in (10) instead of $G_c$ is due to the mathematical requirements of the Statistical Wave Field Theory. Indeed, in places our calculations of second order statistics will involve the square of function $\widehat{G}_0(\boldsymbol{k}, k)$ in (12). The problem with the complex Green's function $G_c$ is that its 3D Fourier transform over space $\widehat{G}_c(\boldsymbol{k}, k)$ is not a function but rather a Radon measure, so that its square is not defined mathematically, whereas the square of function $\widehat{G}_0(\boldsymbol{k}, k)$ in (12) is mathematically well-defined[4].

Fortunately, the fact that we consider a free-field Green's function $G_0$ that does not satisfy the Sommerfeld radiation condition will not prevent us from calculating the correct

[3]This condition enforces the causality of the inverse 1D-Fourier transform (1) of $f \mapsto G_c(\boldsymbol{x}, \boldsymbol{x}_0, \frac{f}{c})$ in the time domain.

[4]Actually, $G_0$ is the only free-field Green's function whose squared 3D Fourier transform is mathematically well-defined.

expression of the causal source response. Similarly, in the presence of boundaries, and in both cases of Neumann and Robin's conditions, we will also consider Green's functions $G$ such that the inverse 1D-Fourier transform (1) of $f \mapsto G(\boldsymbol{x}, \boldsymbol{x}_0, \frac{f}{c})$ is not causal. Again, this will not prevent us from calculating the correct expression of the causal source response.

*3.2. B-function*

Let us now introduce the main calculus tool that we will use in this paper: the $B$-function. In the case of a domain $V \subset \mathbb{R}^3$ with boundaries, any Green's function $G(\boldsymbol{x}, \boldsymbol{x}_0, k)$ can generally be analytically continued on a mathematical vicinity $\mathcal{D}$ of $V$, which depends on the geometry and the specific admittance of the boundary surface. In some cases, this extension holds in the full space $\mathcal{D} = \mathbb{R}^3$: for instance, it is well known that the Green's function of the cuboid in the case of Neumann's boundary condition can be described with a periodic discrete set of image sources (Allen and Berkley, 1979), and this parametrization extends analytically to $\mathbb{R}^3$. The extension to $\mathbb{R}^3$ also holds in the case of a half-space $V$ with a plane boundary, both for the Neumann's boundary condition (Section 3.3.1) and for the Robin's boundary condition when the specific admittance $\widehat{\beta} \in \mathbb{C}$ has a negative imaginary part (Section 3.4.1).

We then define the $B$-function on $\mathcal{D} \subseteq \mathbb{R}^3$ as:

$$B(\boldsymbol{y}, \boldsymbol{x}_0, k) = -\left(\Delta G(\boldsymbol{y}, \boldsymbol{x}_0, k) + 4\pi^2 k^2 G(\boldsymbol{y}, \boldsymbol{x}_0, k)\right). \tag{13}$$

By definition of the Green's function $G$ in (7), the restriction of the $B$-function to $V$ is $\delta(\boldsymbol{y} - \boldsymbol{x}_0)$. Note that, even though there is possibly an infinity of Green's functions $G$, all of them lead to the same unique $B$-function[5].

Reciprocally, when $\mathcal{D} = \mathbb{R}^3$, a particular Green's function $G$ is obtained as:

$$G(\boldsymbol{x}, \boldsymbol{x}_0, k) = \int_{\boldsymbol{y} \in \mathbb{R}^3} G_0(\boldsymbol{x} - \boldsymbol{y}, k)\, B(\boldsymbol{y}, \boldsymbol{x}_0, k) d\boldsymbol{y} \tag{14}$$

where $G_0$ is the real free-field Green's function defined in (10). Equation (14) permits us to interpret the $B$-function as a spatial distribution of image sources in the free field, which collectively generate inside $V$ the same response as that of the single original source within the bounded domain $V$.

Note that both in the free field and in the presence of a boundary with Neumann's boundary condition, the $B$-function is actually independent of $k$. In this case, we will just denote it $B(\boldsymbol{y}, \boldsymbol{x}_0)$.

*3.3. Neumann's boundary condition*

We consider a simply connected domain $V \subsetneq \mathbb{R}^3$, whose boundary $\partial V$ is a Lipschitz continuous and almost everywhere (a.e.) continuously differentiable two-dimensional manifold.

[5] Indeed, given two Green's functions $G_1$ and $G_2$ and their image source distributions $B_1$ and $B_2$, $G_1 - G_2$ is an analytic function which is a solution to the homogeneous Helmholtz equation on $V$, so it is also a solution to the homogeneous Helmholtz equation on $\mathcal{D}$, therefore $B_1 - B_2$ is zero on $\mathcal{D}$.

Neumann's boundary condition of the wave equation (3) states that

$$\forall t \in \mathbb{R},\, \forall \boldsymbol{x} \in \partial V,\; \frac{\partial p(\boldsymbol{x}, t)}{\partial \boldsymbol{n}(\boldsymbol{x})} = 0, \tag{15}$$

where $\partial V$ denotes the boundary surface of $V$, and $\frac{\partial}{\partial \boldsymbol{n}(\boldsymbol{x})}$ denotes partial differentiation in the direction of the outward normal to this surface at $\boldsymbol{x}$. With the Helmholtz equation (4), condition (15) becomes

$$\forall \boldsymbol{x} \in \partial V,\; \frac{\partial \phi(\boldsymbol{x})}{\partial \boldsymbol{n}(\boldsymbol{x})} = 0. \tag{16}$$

In room acoustics, equations (15) and (16) model the reflection of sound waves by *hard* (or *rigid*) surfaces, which reflect the wave without absorbing any energy (Kuttruff, 2014, Chapter 3).

*3.3.1. Plane boundary*

Suppose that $V$ is a half-space delimited by a plane boundary $\partial V$, so that the outward normal vector $\boldsymbol{n}(\boldsymbol{x}) = \boldsymbol{n}$ is uniform on the boundary. Without loss of generality, we assume that $\partial V$ contains the origin of space, and we denote $\boldsymbol{S}_{\partial V} = \boldsymbol{I} - 2\boldsymbol{n}\,\boldsymbol{n}^\top$ the $3 \times 3$ matrix of the reflection symmetry w.r.t. plane $\partial V$. Then given a punctual source position $\boldsymbol{x}_0 \in \mathring{V}$, a Green's function of the Helmholtz equation (4) is expressed as

$$G(\boldsymbol{x}, \boldsymbol{x}_0, k) = G_0(\boldsymbol{x} - \boldsymbol{x}_0, k) + G_0(\boldsymbol{x} - \boldsymbol{S}_{\partial V}\boldsymbol{x}_0, k) \tag{17}$$

where $G_0$ was defined in (10). Indeed, function $G$ in (17) is a solution to the inhomogeneous Helmholtz equation (7) in $V$ and satisfies the boundary condition (16) on $\partial V$.

Note that (17) is formally identical to (14), where the $B$-function is a Radon measure on $\mathcal{D} = \mathbb{R}^3$ that describes the spatial distribution of two sources, one at the original source position $\boldsymbol{x}_0 \in \mathring{V}$, and one at a so-called *image source* position $\boldsymbol{S}_{\partial V}\boldsymbol{x}_0$, which lies outside the domain $V$:

$$B\left(\boldsymbol{y}, \boldsymbol{x}_0\right) = \delta(\boldsymbol{y} - \boldsymbol{x}_0) + \delta(\boldsymbol{y} - \boldsymbol{S}_{\partial V}\boldsymbol{x}_0). \tag{18}$$

*3.3.2. Simply connected compact domain*

If $V$ is a compact domain (i.e. bounded and closed), then the Sturm-Liouville theory (Pearson, 2001) shows that the set of *eigenvalues* $k_n$ and unit *eigenfunctions* $\phi_n(\boldsymbol{x})$, also called *normal modes*, that are solutions to (4) and (16) is discrete: it is indexed by $n \in \mathbb{N}$. Moreover, both $k_n$ and $\phi_n(\boldsymbol{x})$ are real. So without loss of generality, the eigenvalues $k_n$ can be assumed nonnegative and sorted by non-decreasing order. Finally, the set $\{\phi_n(\boldsymbol{x})\}_{n\in\mathbb{N}}$ is such that

$$\forall \boldsymbol{x}, \boldsymbol{y} \in V,\; \sum_{n\in\mathbb{N}} \phi_n(\boldsymbol{x})\phi_n(\boldsymbol{y}) = \delta(\boldsymbol{x} - \boldsymbol{y}). \tag{19}$$

This set forms a Hilbert basis of the real Hilbert space $L^2(V)$ of square-integrable functions on $V$. In addition, note that the constant function $\phi_0(\boldsymbol{x}) = \frac{1}{\sqrt{|V|}}$ is always an eigenfunction of (4) and (16), of eigenvalue $k_0 = 0$.

Then given a punctual source position $\boldsymbol{x}_0 \in \mathring{V}$, we consider the following Green's function of the Helmholtz equation (4):

$$G(\boldsymbol{x}, \boldsymbol{x}_0, k) = \sum_{n \in \mathbb{N}} \frac{\phi_n(\boldsymbol{x}_0)\, \phi_n(\boldsymbol{x})}{4\pi^2(k_n^2 - k^2)}. \tag{20}$$

Indeed, equation (19) shows that function $G$ in (20) is a solution to the inhomogeneous Helmholtz equation (7) in $V$, and it satisfies the boundary condition (16) on $\partial V$ because all functions $\phi_n(\boldsymbol{x})$ satisfy this condition.

Then, by substituting equation (20) into (8), we get $\forall \boldsymbol{x} \in V$, $\forall t \in \mathbb{R}$,

$$\dot{g}(\boldsymbol{x}, \boldsymbol{x}_0, t) = -c^2 \sum_{n \in \mathbb{N}} \int_{f \in \mathbb{R}} \frac{\phi_n(\boldsymbol{x}_0)\, \phi_n(\boldsymbol{x})}{4\pi^2(f^2 - c^2 k_n^2)}\, 2\imath\pi f\, e^{2\imath\pi f t} df. \tag{21}$$

We note that $\forall n \in \mathbb{N}^*$, the integrand in the integral over $f$ in (21) has two real poles, one at $f = ck_n$ and one at $f = -ck_n$. In addition, for $n = 0$, $k_0 = 0$ and the integrand has a simple pole at $f = 0$. By applying the residue theorem (Ahlfors, 1979) to (21), we get a simplified expression of $\dot{g}(\boldsymbol{x}, \boldsymbol{x}_0, t)$:

$$\dot{g}(\boldsymbol{x}, \boldsymbol{x}_0, t) = \frac{c^2}{2} \operatorname{sign}(t) \sum_{n \in \mathbb{N}} \phi_n(\boldsymbol{x}_0)\, \phi_n(\boldsymbol{x}) \cos(2\pi c k_n t).$$

Then, by noticing that function $\dot{g}(\boldsymbol{x}, \boldsymbol{x}_0, t)$ is again an odd function of time, the expression of the source response $p$ is still given by (11). We thus get $\forall \boldsymbol{x} \in V$, $\forall t \in \mathbb{R}$,

$$p(\boldsymbol{x}, \boldsymbol{x}_0, t) = H(t)\, q(\boldsymbol{x}, \boldsymbol{x}_0, t), \tag{22}$$

where $q(\boldsymbol{x}, \boldsymbol{x}_0, t)$ is defined as

$$q(\boldsymbol{x}, \boldsymbol{x}_0, t) = c^2 \sum_{n \in \mathbb{N}} \phi_n(\boldsymbol{x}_0)\, \phi_n(\boldsymbol{x}) \cos(2\pi c\, k_n t). \tag{23}$$

It can be readily verified that function $p$ in (22) with $q$ as in (23) is the unique causal solution to the inhomogeneous wave equation (5) in $V$ which satisfies the boundary condition (15) on $\partial V$.

In other respects, for any eigenvalue $k$, the projection $\sum_{k_n = k} \phi_n(\boldsymbol{x}_0)\, \phi_n(\boldsymbol{y})$ onto the corresponding eigenspace is an analytic function of $\boldsymbol{x}_0$ and $\boldsymbol{y} \in V$, so it can generally be continued as an analytic function on a mathematical vicinity $\mathcal{D}$ of $V$, which is a solution to the Helmholtz equation (4) on $\mathcal{D}$. By substituting (20) into (13), we get the closed-form expression of the $B$-function on $\mathcal{D}$:

$$B(\boldsymbol{y}, \boldsymbol{x}_0) = \sum_{n \in \mathbb{N}} \phi_n(\boldsymbol{x}_0)\, \phi_n(\boldsymbol{y}). \tag{24}$$

We note that equation (19) confirms that the restriction of the $B$-function to $V$ is $\delta(\boldsymbol{y} - \boldsymbol{x}_0)$, as already mentioned in Section 3.2.

*3.4. Robin's boundary condition*

We still consider a simply connected domain $V \not\subseteq \mathbb{R}^3$, whose boundary $\partial V$ is a Lipschitz continuous and a.e. continuously differentiable two-dimensional manifold. Now, the boundary $\partial V$ is characterized by the *specific admittance* $\widehat{\beta}(\boldsymbol{x}, k) \in \mathbb{C}$, which is an a.e. continuous function of the position $\boldsymbol{x} \in \partial V$. Let $\beta(\boldsymbol{x}, \tau)$ denote the time-domain *specific conductance*, which is the inverse 1D Fourier transform (1) of $f \mapsto \widehat{\beta}(\boldsymbol{x}, \frac{f}{c})$. Then the boundary condition of the wave equation (3) becomes

$$\forall \boldsymbol{x} \in \partial V, \ \frac{\partial p(\boldsymbol{x}, t)}{\partial \boldsymbol{n}(\boldsymbol{x})} + \beta(\boldsymbol{x}, .) \overset{t}{*} \frac{1}{c} \frac{\partial p(\boldsymbol{x}, t)}{\partial t} = 0, \tag{25}$$

where $\overset{t}{*}$ denotes the convolution product over time $t$.

With the Helmholtz equation (4), condition (25) becomes:

$$\forall \boldsymbol{x} \in \partial V, \ \frac{\partial \varphi(\boldsymbol{x}, k)}{\partial \boldsymbol{n}(\boldsymbol{x})} + 2\imath\pi k \widehat{\beta}(\boldsymbol{x}, k) \varphi(\boldsymbol{x}, k) = 0. \tag{26}$$

Note that the boundary condition now explicitly depends on the wave number $k$, so the solutions to the homogeneous Helmholtz equation also depend on $k$, thus (4) has to be rewritten

$$\Delta \varphi(\boldsymbol{x}, k) + 4\pi^2 \kappa(k)^2 \varphi(\boldsymbol{x}, k) = 0 \tag{27}$$

where the wave number is now denoted $\kappa(k) \in \mathbb{C}$.

In room acoustics, equations (25) and (26) permit us to model the reflection of sound waves by *non-rigid* surfaces, which absorb a part of the energy of the incident wave (Kuttruff, 2014, Chapter 3). In this case the real part of the specific admittance $\widehat{\beta}(\boldsymbol{x}, k)$ is positive, and the specific conductance $\beta(\boldsymbol{x}, \tau)$ is real and causal. Moreover, it is assumed that the room has *locally reacting* boundary surfaces, which means that $\widehat{\beta}(\boldsymbol{x}, k)$ depends only on the position $\boldsymbol{x}$ over the boundary surface and on the wave number $k$, but not on the angle of sound incidence (Kuttruff, 2014, Chapter 2), so $\widehat{\beta}$ does not depend on the *orientation* of the wave vector $\boldsymbol{k}$, but only on its norm. The relationship between the specific admittance and the physical properties of various realistic materials, as well as experimental methods for measuring $\widehat{\beta}$, are described in (Kuttruff, 2014, Chapters 2 and 8).

Under these assumptions, the absorption coefficient of the material at the boundary surface, i.e. the ratio of energy of the incoming wave which is absorbed by the material, is related to the specific admittance as follows, *cf.* (Morse and Ingard, 1968, Page 580) and (Kuttruff, 2014, Chapter 2):

$$a(\boldsymbol{s}, f, u) = 1 - \left| \frac{u - \widehat{\beta}(\boldsymbol{s}, \frac{f}{c})}{u + \widehat{\beta}(\boldsymbol{s}, \frac{f}{c})} \right|^2. \tag{28}$$

In (28), $a(\boldsymbol{s}, f, u)$ denotes the absorption coefficient for an incident plane wave of frequency $f$, whose direction forms an angle $\theta \in [0, \frac{\pi}{2}]$ with the outward normal $\boldsymbol{n}(\boldsymbol{s})$ to the boundary at point $\boldsymbol{s}$, such that $u = \cos(\theta) \geq 0$. In particular, $u = 1$ corresponds to normal incidence, i.e. $\theta = 0$. Note that the inequality $\mathrm{Re}(\widehat{\beta}(\boldsymbol{x}, k)) \geq 0$ guarantees that $0 \leq a(\boldsymbol{s}, f, u) \leq 1$.

*3.4.1. Plane boundary*

As in Section 3.3.1, suppose that $V$ is a half-space delimited by a plane boundary $\partial V$, so that the outward normal vector $\boldsymbol{n}(\boldsymbol{x}) = \boldsymbol{n}$ is uniform on the boundary. Again, without loss of generality, we assume that $\partial V$ contains the origin of space, and we denote $\boldsymbol{S}_{\partial V} = \boldsymbol{I} - 2\boldsymbol{n}\,\boldsymbol{n}^\top$ the $3 \times 3$ matrix of the reflection symmetry w.r.t. plane $\partial V$, and $\boldsymbol{P}_{\partial V}$ any $3 \times 2$ matrix whose columns form an orthonormal basis of $\partial V$.

Let us now assume that the specific admittance $\widehat{\beta}(\boldsymbol{x}, k) = \widehat{\beta}(k)$ is constant on the boundary plane, and that $\mathrm{Im}(\widehat{\beta}(k)) < 0$. Then given a punctual source position $\boldsymbol{x}_0 \in \mathring{V}$, a Green's function $G$ of the Helmholtz equation (4) can be expressed as in (14), where $G_0$ was defined in (10), and the $B$-function defined on $\mathcal{D} = \mathbb{R}^3$ now depends on $k$:

$$\begin{aligned} B(\boldsymbol{y}, \boldsymbol{x}_0, k) = \;& \delta(\boldsymbol{y} - \boldsymbol{x}_0) + \delta(\boldsymbol{y} - \boldsymbol{S}_{\partial V}\boldsymbol{x}_0) \\ & -4\imath\pi k\widehat{\beta}(k) H(\boldsymbol{n}^\top(\boldsymbol{y} + \boldsymbol{x}_0)) e^{-2\imath\pi k\widehat{\beta}(k)\boldsymbol{n}^\top(\boldsymbol{y}+\boldsymbol{x}_0)} \delta(\boldsymbol{P}_{\partial V}^\top(\boldsymbol{y} - \boldsymbol{x}_0)). \end{aligned} \tag{29}$$

Indeed, the restriction of function $B(\boldsymbol{y}, \boldsymbol{x}_0, k)$ in (29) to $\boldsymbol{y} \in V$ is $\delta(\boldsymbol{y} - \boldsymbol{x}_0)$, which shows that $G$ is a solution to the inhomogeneous Helmholtz equation (7). Moreover, the 3D Fourier transform (2) of $B(\boldsymbol{y}, \boldsymbol{x}_0, k)$ is[6]

$$\widehat{B}(\boldsymbol{\kappa}, \boldsymbol{x}_0, k) = e^{-2\imath\pi\boldsymbol{\kappa}^\top\boldsymbol{x}_0} + \frac{\boldsymbol{n}^\top\boldsymbol{\kappa} - k\widehat{\beta}(k)}{\boldsymbol{n}^\top\boldsymbol{\kappa} + k\widehat{\beta}(k)} e^{-2\imath\pi\boldsymbol{\kappa}^\top\boldsymbol{S}_{\partial V}\boldsymbol{x}_0}, \tag{30}$$

so the Green's function $G(\boldsymbol{x}, \boldsymbol{x}_0, k)$ can be written as the inverse 3D Fourier transform (2) of $\widehat{G}(\boldsymbol{\kappa}, \boldsymbol{x}_0, k)$:

$$\begin{aligned} G(\boldsymbol{x}, \boldsymbol{x}_0, k) = & \int_{\boldsymbol{\kappa}\in\mathbb{R}^3} \frac{e^{2\imath\pi\boldsymbol{\kappa}^\top(\boldsymbol{x}-\boldsymbol{x}_0)} + \frac{\boldsymbol{n}^\top\boldsymbol{\kappa}-k\widehat{\beta}(k)}{\boldsymbol{n}^\top\boldsymbol{\kappa}+k\widehat{\beta}(k)} e^{2\imath\pi\boldsymbol{\kappa}^\top(\boldsymbol{x}-\boldsymbol{S}_{\partial V}\boldsymbol{x}_0)}}{4\pi^2(\|\boldsymbol{\kappa}\|_2^2 - k^2)} d\boldsymbol{\kappa} \\ = & \int_{\boldsymbol{\kappa}\in\mathbb{R}^3} \frac{e^{2\imath\pi\boldsymbol{\kappa}^\top(\boldsymbol{x}-\boldsymbol{x}_0)} + \frac{\boldsymbol{n}^\top\boldsymbol{\kappa}+k\widehat{\beta}(k)}{\boldsymbol{n}^\top\boldsymbol{\kappa}-k\widehat{\beta}(k)} e^{2\imath\pi\boldsymbol{\kappa}^\top(\boldsymbol{S}_{\partial V}\boldsymbol{x}-\boldsymbol{x}_0)}}{4\pi^2(\|\boldsymbol{\kappa}\|_2^2 - k^2)} d\boldsymbol{\kappa} \end{aligned} \tag{31}$$

where we have substituted the 3D Fourier transform of (14), as well as (12) and (30), in the first equality, and we have applied the change of variable $\boldsymbol{\kappa} \mapsto \boldsymbol{S}_{\partial V}\boldsymbol{\kappa}$ to the second term in the second equality. Then it can be easily verified from (31) that $G$ satisfies the boundary condition (26) on $\partial V$.

The $B$-function in (29) is still a Radon measure, but this time it contains not only two discrete atoms (the original source at $\boldsymbol{x}_0 \in \mathring{V}$ and its image at $\boldsymbol{S}_{\partial V}\boldsymbol{x}_0$), but also a continuum of image sources located outside $V$.

When $\mathrm{Im}(\widehat{\beta}(k)) > 0$, the Green's function can still be expressed in analytic form: a parametrization of $G$, which holds $\forall\,\mathrm{Im}(\widehat{\beta}(k)) \in \mathbb{R}$, was presented in (Ochmann, 2004), where image sources are distributed in a complex space domain. However, $G$ can no longer be analytically continued on $\mathbb{R}^3$, so the $B$-function is no longer defined on $\mathbb{R}^3$, and $G$ can no longer be expressed as in (14).

[6]In the case of Robin's boundary condition, the wave vector will be denoted $\boldsymbol{\kappa}$ instead of $\boldsymbol{k}$ which is used in the Neumann case, in order to avoid any confusion in Section 6, where the two notations will coexist.

*3.4.2. Simply connected compact domain*

If $V$ is a compact domain (i.e. bounded and closed), then the set of eigenvalues $\kappa_n(k)$ and eigenfunctions $\varphi_n(\boldsymbol{x}, k)$ that are solutions to (26) and (27) is still discrete and indexed by $n \in \mathbb{N}$. Moreover, at $k = 0$ the boundary condition (26) is the same as (16), so we get $\kappa_n(0) = k_n$ and $\varphi_n(\boldsymbol{x}, 0) = \phi_n(\boldsymbol{x})$. When $k \neq 0$, $\widehat{\beta}(\boldsymbol{x}, k)$ is complex and $\mathrm{Re}(\widehat{\beta}(\boldsymbol{x}, k)) > 0$. Then both $\kappa_n(k)$ and $\varphi_n(\boldsymbol{x}, k)$ are complex and $\mathrm{Im}(\kappa_n(k)) > 0$. In addition, similarly to equation (19), the set $\{\varphi_n(\boldsymbol{x}, k)\}_{n\in\mathbb{N}}$ is such that

$$\forall \boldsymbol{x}, \boldsymbol{y} \in V, \sum_{n\in\mathbb{N}} \varphi_n(\boldsymbol{x}, k)\varphi_n(\boldsymbol{y}, k) = \delta(\boldsymbol{x} - \boldsymbol{y}). \tag{32}$$

Because this set is not orthogonal w.r.t. the Hermitian inner product, it does not form a Hilbert basis of the complex Hilbert space $L^2(V)$, but it still forms an Abel basis of $L^2(V)$ (Bögli *et al.*, 2022).

Finally, by changing the sign of $k$ in (26) and (27), we get $\varphi_n(\boldsymbol{x}, -k) = \overline{\varphi_n(\boldsymbol{x}, k)}$ and $\kappa_n(-k) = -\overline{\kappa_n(k)}$ (since both $\kappa_n(k)$ and $\kappa_n(-k)$ have a positive imaginary part). So without loss of generality, at fixed $k \in \mathbb{R}$, the eigenvalues $\kappa_n(k)$ can be assumed to have a real part of the same sign of $k$ $\forall n \in \mathbb{N}$.

Then given a punctual source position $\boldsymbol{x}_0 \in \mathring{V}$, a Green's function of the Helmholtz equation (4) is expressed as

$$G(\boldsymbol{x}, \boldsymbol{x}_0, k) = \sum_{n\in\mathbb{N}} \frac{\varphi_n(\boldsymbol{x}_0, k)\, \varphi_n(\boldsymbol{x}, k)}{4\pi^2(\kappa_n(k)^2 - k^2)}. \tag{33}$$

Indeed, equation (32) shows that function $G$ in (33) is a solution to the inhomogeneous Helmholtz equation (7) in $V$, and it satisfies the boundary condition (26) on $\partial V$ because all functions $\varphi_n(\boldsymbol{x}, k)$ satisfy this condition.

Then, by substituting equation (33) into (8), we get $\forall \boldsymbol{x} \in V$, $\forall t \in \mathbb{R}$,

$$\dot{g}(\boldsymbol{x}, \boldsymbol{x}_0, t) = -c^2 \sum_{n\in\mathbb{N}} \int_{f\in\mathbb{R}} \frac{\varphi_n(\boldsymbol{x}_0, \frac{f}{c})\, \varphi_n(\boldsymbol{x}, \frac{f}{c})}{4\pi^2 \left(f^2 - c^2\kappa_n(\frac{f}{c})^2\right)}\, 2\imath\pi f\, e^{2\imath\pi f t} df. \tag{34}$$

The integral in (34) can then be calculated by means of the residue theorem. Indeed, suppose that $\forall n \in \mathbb{N}^*$, a root of the equation $\frac{f}{c} = \kappa_n(\frac{f}{c})$ is $\nu_n = f_n + \imath\gamma_n$ with $f_n, \gamma_n > 0$. Then because of the symmetry property $\kappa_n(-\overline{k}) = -\overline{\kappa_n(k)}$, there will be another root at $-\overline{\nu_n} = -f_n + \imath\gamma_n$. Thus the integrand in the right member of (34) has two simple poles at $f = \nu_n$ and $f = -\overline{\nu_n}$. In addition, for $n = 0$, $\kappa_0(0) = k_0 = 0$, thus the integrand has a simple pole at $f = \nu_0 = 0$.

Then applying the residue theorem to (34) leads to the equivalent expression[7]:

$$\dot{g}(\boldsymbol{x}, \boldsymbol{x}_0, t) = c^2 \left( \tfrac{\lambda}{2} \operatorname{sign}(t) + H(t) \operatorname{Re} \left( \sum_{n \in \mathbb{N}^*} \varphi_n(\boldsymbol{x}_0, \tfrac{\nu_n}{c})\, \varphi_n(\boldsymbol{x}, \tfrac{\nu_n}{c}) e^{2\imath\pi\nu_n t} \right) \right), \tag{35}$$

where $\lambda \triangleq \frac{1}{|V|}$. The causal source response $p$ is related to $\dot{g}$ by adding the constant term $\frac{\lambda c^2}{2}$, which is a solution to the homogeneous wave equation (3) with the boundary condition (25):

$$p(\boldsymbol{x}, \boldsymbol{x}_0, t) = \dot{g}(\boldsymbol{x}, \boldsymbol{x}_0, t) + \tfrac{\lambda c^2}{2}. \tag{36}$$

By substituting (35) into (36), we retrieve (22), with

$$q(\boldsymbol{x}, \boldsymbol{x}_0, t) = c^2 \operatorname{Re} \left( \sum_{n \in \mathbb{N}} \varphi_n(\boldsymbol{x}_0, \tfrac{\nu_n}{c})\, \varphi_n(\boldsymbol{x}, \tfrac{\nu_n}{c}) e^{2\imath\pi\nu_n t} \right). \tag{37}$$

Note that equation (37) generalizes (23) which we obtained in the case of Neumann's boundary condition, to complex eigenfunctions $\varphi_n$ and complex frequencies $\nu_n$.

In other respects, for any eigenvalue $\kappa$, the projection $\sum_{\kappa_n(k)=\kappa} \varphi_n(\boldsymbol{x}_0, k)\, \varphi_n(\boldsymbol{y}, k)$ onto the corresponding eigenspace is an analytic function of $\boldsymbol{x}_0$ and $\boldsymbol{y} \in V$, so it can generally be continued as an analytic function on a mathematical vicinity $\mathcal{D}$ of $V$, which is a solution to the Helmholtz equation (27) on $\mathcal{D}$. By substituting (27) and (33) into (13), we get the closed-form expression of the $B$-function on $\mathcal{D}$:

$$B(\boldsymbol{y}, \boldsymbol{x}_0, k) = \sum_{n \in \mathbb{N}} \varphi_n(\boldsymbol{x}_0, k)\, \varphi_n(\boldsymbol{y}, k). \tag{38}$$

Again, we note that equation (32) confirms that the restriction of the $B$-function to $V$ is $\delta(\boldsymbol{y} - \boldsymbol{x}_0)$.

### *3.5. Distribution of the discrete normal modes*

We have seen in Sections 3.3.2 and 3.4.2 that in a simply connected compact domain, the set of normal modes of the Helmholtz equation is discrete and countable. Note that in Section 3.3, the wave number was denoted $k$, whereas in Section 3.4, it was denoted $\kappa$, which actually depends on $k$, as in equation (27). From now on, we will stick to the $\kappa$ notation that we used for Robin's boundary condition, because it is more general, since it includes Neumann's boundary condition as a particular case: indeed, when $k = 0$, (26) reduces to (16).

---

[7]Actually, the expression in (35) is incomplete, because function $\varphi_n(\boldsymbol{x}_0, \frac{f}{c})\, \varphi_n(\boldsymbol{x}, \frac{f}{c})$ in the numerator of the fraction in (34) is a meromorphic function of $f$, with its own singularities. These singularities are generally ignored by theoretical acousticians, *cf.* (Morse and Ingard, 1968, Chapter 9), which amounts to assume that they are located in a region of the complex plane which is above the set of poles $\cup_{n \in \mathbb{N}} \{\nu_n, -\overline{\nu_n}\}$, so that they generate terms in $\dot{g}(\boldsymbol{x}, \boldsymbol{x}_0, t)$ that decay faster than the complex exponentials $e^{2\imath\pi\nu_n t}$ in (35).

*3.5.1. Asymptotic expansion of the modal density*

It is well-known that the density of modes is quadratically increasing with the wave number $\kappa$, so when the frequency is high enough, the spectrum is well described by a smooth density function $\rho(\kappa, k)$. When the boundary surface of the domain $V$ is smooth enough, Balian and Bloch (1970) have shown that function $\rho(\kappa, k)$ admits the following first order expansion[8] when $\kappa \to +\infty$:

$$\rho(\kappa, k) = 4\pi|V|\kappa^2 + \kappa \int_{\boldsymbol{s}\in\partial V} \left(\tfrac{\pi}{2} + 2\arctan\left(\tfrac{k}{\kappa}\operatorname{Im}\left(\widehat{\beta}(\boldsymbol{s}, k)\right)\right)\right) dS(\boldsymbol{s}) + O(1). \tag{39}$$

This equation holds both in the case of Neumann's boundary condition, which corresponds to $k = 0$ as mentioned previously, and in the case of Robin's boundary condition if and only if $\widehat{\beta}$ is purely imaginary[9]. In the right member of equation (39), the dominant term $4\pi|V|\kappa^2$ is known as the *volume term*. The first order term, which involves an integral over the boundary surface, is called the *surface term*. Note that the original equation from (Balian and Bloch, 1970) also includes a second order term called the *curvature term*, that we will exploit and generalize in future papers (see Section 7).

In room acoustics, a purely imaginary specific admittance $\widehat{\beta}$ corresponds to reactive surfaces, which are free of absorption. If $\operatorname{Im}(\widehat{\beta}) < 0$, which indicates that the motion of the surface is mass-controlled, then the eigenvalues $\kappa_n(k)$ are real-valued and *increased* w.r.t. the eigenvalues $k_n$ of the rigid-walled room, in a way that turns the modal density $\rho(\kappa, 0)$ into $\rho(\kappa, k)$ as in (39). Conversely, if $\operatorname{Im}(\widehat{\beta}) > 0$, which characterizes a compliance surface, i.e. a surface with the impedance of a spring, then the eigenvalues $\kappa_n(k)$ are real-valued and *lowered* w.r.t. the eigenvalues $k_n$ of the rigid-walled room, and the resulting modification of the modal density is again described by (39).

A few applications of (39) to different kinds of waves are mentioned in (Balian and Bloch, 1970): in nuclear physics, the Helmholtz equation describes the actual self-consistent field of a heavy nucleus, and the distribution of its eigenvalues in (39) provides a description of the nuclear properties in terms of the deformation; in electromagnetic theory, the distribution of normal modes of electromagnetic waves in a cavity permits for instance to evaluate the Casimir effect, considered as the sum of the energy shifts of the electromagnetic eigenmodes due to the presence of a conductor.

We will explain in Sections 4 to 6 how the asymptotic expansion in equation (39) is related to the Statistical Wave Field Theory. In particular, the mathematical developments in (Balian and Bloch, 1970) are based on a multiple reflection expansion of the Green's function $G$. Similarly, our mathematical developments will be based on a multiple reflection expansion of the $B$-function introduced in Section 3.2.

As explained in (Balian and Bloch, 1970, Page 435), equation (39) does not hold when

[8]In equation (39), we have modified the notation used in (Balian and Bloch, 1970) so as to adapt it to the notation used in this paper.

[9]Indeed, this assumption is necessary to guarantee that the eigenvalues $\kappa_n(k)$ are real, in order to be able to define a density function $\rho(\kappa, k)$ over $\mathbb{R}$.

$\widehat{\beta} \approx 1$ (which corresponds to a completely absorbent surface at normal incidence), so this value will be also excluded in the Statistical Wave Field Theory.

### *3.5.2. Oscillations of the modal density*

Equation (39) implicitly involves a smoothing kernel acting in the spectral domain, which turns the discrete distribution of modes into a smooth modal density. When the width of this smoothing kernel becomes small, fluctuations appear in the modal density, which actually oscillates around the smooth function $\kappa \mapsto \rho(\kappa, k)$ predicted by (39). Unfortunately, these oscillations depend in a complicated way on the domain's global geometry, and cannot be described by means of a simple general closed-form expression such as (39).

In (Balian and Bloch, 1972), a systematic investigation of these fluctuations proved that the dominant oscillations are associated with the shortest *closed stationary paths*, i.e., the closed polygons inscribed in the boundary surface $\partial V$, having their vertices on $\partial V$ and such that mirror reflections on $\partial V$ (i.e. specular reflections as in geometric acoustics and optics) take place at each vertex. An extreme case of fluctuating modal density appears when $\partial V$ is a sphere: the oscillations are then of order 1 in (39), preventing the asymptotic expansion from being carried out beyond the first order *surface term*. In this case, the closed stationary paths are the regular polygons in diametrical planes of the sphere (ordinary or starred polygons).

In room acoustics,, as explained in (Balian and Bloch, 1972), the design of concert halls requires us to minimize these oscillations, since they tend to emphasize some frequencies with respect to the others. An elementary rule to follow for this purpose is to avoid shapes favoring the existence of closed stationary paths.

Since the *power spectrum* of the Statistical Wave Field Theory (that will be introduced in Section 4.4) is related to the asymptotic expansion of the modal density in (39), one could expect it to be prone to the same problem of fluctuations. However, the Statistical Wave Field Theory as it is presented in this paper is based on the *mixing* assumption (that will be introduced in Section 3.6.1), which precisely implies that the domain's shape is such that closed stationary paths are negligible. Therefore the fluctuations are also negligible, and the asymptotic expansion can be carried out up to the second order terms, including the previously-mentioned *curvature* term. As a counterexample, the sphere is known as a typical example of non-mixing billiard (Polack, 1992). Therefore non-mixing geometric shapes such as the sphere are excluded in the Statistical Wave Field Theory.

### *3.6. Review of known statistical properties in room acoustics*

In room acoustics, a room impulse response is made of a first impulse, which corresponds to the direct path between the source and the receiver, followed by a succession of reflections on the room boundary, whose density increases quadratically over time. It is well known that after many reflections, i.e. after a time which is known as the *transition time* or *mixing time*, and at high frequency, the collective behavior of the reflected waves becomes stochastic, a physical phenomenon that is called *late reverberation*. In the literature, several works aimed to model various aspects of this stochastic behavior. We summarize here a few important contributions, which are closely related to the Statistical Wave Field Theory.

*3.6.1. Reverberation as a dynamical billiard*

We have seen in Section 3.5.1 that when the frequency is high enough, the spectrum of the source response can be considered continuous. Moreover, at high frequency, it is well known that wave propagation can be approximated by considering the trajectory of rays which undergo successive specular reflections on the domain boundary, similarly to optical rays (Kuttruff, 2014, Chapter 4). The ray trajectory can then be interpreted as a dynamical billiard which, depending on the boundary geometry, may follow different statistical properties (Polack, 1992). In particular, a dynamical billiard is *ergodic* when over time $t$, the position $\boldsymbol{x}(t)$ and the unit direction vector $\boldsymbol{d}(t)$ of the ray are jointly uniformly distributed in the *phase space* $V \times \mathcal{S}(0,1)$, where $\mathcal{S}(0,1)$ denotes the unit sphere. A stronger statistical property, *mixing*, can be formulated in the following way: if the *source* corresponds to time 0 and the *receiver* corresponds to time $T$, then in addition to their uniform distribution in the phase space, when the elapsed time $T$ is long enough, the receiver's position $\boldsymbol{x}(T)$ and direction $\boldsymbol{d}(T)$ are statistically independent of the source's position $\boldsymbol{x}(0)$ and direction $\boldsymbol{d}(0)$. Consequently, in a mixing billiard, the statistics of the reflections undergone by any ray, during an elapsed time $T$ sufficiently long, are defined independently of the source and from the receiver's positions and directions.

In room acoustics, Polack (1992) applied the billiard theory to investigate the properties of the reverberation time in mixing rooms, ergodic rooms, and some non-ergodic rooms. He showed that the classical definition of a *diffuse field* can be considered as equivalent to the mixing property. Theoretically, the mixing and ergodic properties depend on the room's shape in a very complex way, so that there exists no simple geometric characterization of ergodic and mixing rooms. Nevertheless, Polack (1992) mentioned that in practice, most rooms are mixing, even when their shape is theoretically non-mixing: the unavoidable irregularities of a real room's surfaces are sufficient to create mixing conditions in almost any room.

*3.6.2. Reverberation time over frequency*

In room acoustics, the reverberation time, which is often denoted $T_{60}$, is the time it takes for the sound pressure level to reduce by 60 dB. In a diffuse acoustic field, i.e. in a mixing room according to Polack (1992), the early experiments carried out by Wallace Clement Sabine in the late 19th century showed that the reverberation time approximately matches the following empirical law (Joyce, 1975) [10]:

$$T_{60}(f) = \frac{24\ln(10)}{c} \frac{|V|}{\int_{\boldsymbol{s}\in\partial V} a(\boldsymbol{s},f)dS(\boldsymbol{s})} \tag{40}$$

where $a(\boldsymbol{s},f)$ denotes the absorption coefficient of the room surface at point $\boldsymbol{s}$ and frequency $f$, averaged over all directions of incidence. Actually, Sabine's formula only holds

[10] In (40) we have replaced the discrete sum in the formula which is generally presented in the literature by an integral over the boundary surface, and we have explicitly written the dependency on frequency of the absorption coefficient $a$.

in highly reverberant rooms (i.e. when $a(\boldsymbol{s}, f)$ is small). In order to account for larger absorptions, this formula was modified by Carl F. Eyring in 1930:

$$T_{60}(f) = \frac{24\ln(10)}{c} \frac{|V|}{-\int_{\boldsymbol{s}\in\partial V} \ln(1 - a(\boldsymbol{s}, f))dS(\boldsymbol{s})}. \tag{41}$$

Eyring's formula has been both verified experimentally and derived mathematically from a simple probabilistic model (Eyring, 1930). In Section 6.6, we will establish a relationship between Sabine's and Eyring's formulas and the expression of the reverberation time predicted by the Statistical Wave Field Theory.

*3.6.3. Time-frequency distribution*

In his PhD thesis *The transmission of sound energy in rooms*, Jean-Dominique Polack (1988) derived an expression of the Wigner time-frequency distribution[11] of the room impulse response, based on a simple probabilistic model that assigns the same reverberation time to all directions and all frequencies: $\forall t > 0$,

$$W_h(f, t) = B(f)\, e^{-2\alpha t}, \tag{42}$$

where the attenuation coefficient $\alpha$ is related to the reverberation time via $T_{60} = \frac{3\ln(10)}{\alpha}$.

In order to account for the dependency of the attenuation coefficient $\alpha$ on frequency $f$, he also proposed an empirical generalization of (42), which holds in all mixing rooms: $\forall t > 0$,

$$W_h(f, t) = B(f)\, e^{-2\alpha(\frac{f}{c})t}. \tag{43}$$

In Section 6.6, the Statistical Wave Field Theory will permit us to retrieve and to generalize equation (43).

*3.6.4. Spatial correlation over frequency*

In the spectral domain, still in the case of a diffuse acoustic field, i.e. of a mixing room, Cook *et al.* (1955) calculated the correlation of the reverberated wave field between two points $\boldsymbol{x}_1$ and $\boldsymbol{x}_2$ as a function of frequency $f$:

$$\gamma(\boldsymbol{x}_1, \boldsymbol{x}_2, f) = \operatorname{sinc}\left(\frac{2\pi f \|\boldsymbol{x}_1 - \boldsymbol{x}_2\|_2}{c}\right). \tag{44}$$

This formula is remarkably simple and was initially derived from a probabilistic model involving a discrete sum of plane waves coming uniformly from all directions. However, equation (44) only holds when there is no absorption on the room boundary.

In Section 5.4, the Statistical Wave Field Theory will thus permit us to retrieve it in the case of Neumann's boundary condition. In the case of Robin's boundary condition, we will obtain a generalization of (44) which accounts for the non-stationarity of the wave field (see equation (115) in Section 6.4).

[11] The Wigner distribution of a non-stationary random process will be formally defined in Section 4.1.

## 4. Fundamentals of the Statistical Wave Field Theory

The Statistical Wave Field Theory aims to describe mathematically the statistical properties of waves propagating in a bounded domain $V \subset \mathbb{R}^3$. More precisely, it represents the source response $p$ introduced in (5) as a stochastic process, and aims to characterize its probability distribution, especially in terms of the Wigner time-frequency distribution (Section 4.1). When the frequency is high enough (Assumption 2 in Section 4.3), wave propagation can be interpreted as a dynamical billiard, as already explained in Section 3.6.1. In this paper, we focus on the most usual case of mixing billiards[12], so we reformulate the statistical properties of mixing billiards in terms of probabilistic distributions, first of the punctual source position (Assumption 1 in Section 4.2), then of the $B$-function (Assumption 3 in Section 4.4).

### *4.1. Wigner distribution*

In the case of Robin's boundary condition, the source response $p$ will be modeled as a non-stationary random process in Section 6, due to the exponential damping of the normal modes over time (see equation (37)). In signal processing, the standard tool for characterizing the second-order statistics of a non-stationary random process is the *Wigner distribution* (Cohen, 1989), also known as the Wigner-Ville distribution, which describes how the power of this random process is distributed in the time-frequency plane. So let

$$\Gamma_q(\boldsymbol{x}_1, \boldsymbol{x}_2, t_1, t_2) = \text{cov}[q(\boldsymbol{x}_1, t_1), q(\boldsymbol{x}_2, t_2)] \tag{45}$$

denote the *auto-covariance function* (ACF) of a non-stationary random process $q(\boldsymbol{x}, t)$. Its Wigner distribution $W_q$ is defined as follows:

$$\forall f, t \in \mathbb{R},\ W_q(\boldsymbol{x}_1, \boldsymbol{x}_2, f, t) = \int_{\mathbb{R}} \Gamma_q(\boldsymbol{x}_1, \boldsymbol{x}_2, t + \tfrac{\tau}{2}, t - \tfrac{\tau}{2})\, e^{-2\imath\pi f\tau} d\tau. \tag{46}$$

In the same way, the Wigner distribution of a complex function $w(t)$ with $t \in \mathbb{R}$ is defined as:

$$\forall f, t \in \mathbb{R},\ W_w(f, t) = \int_{\mathbb{R}} w(t + \tfrac{\tau}{2})\, \overline{w(t - \tfrac{\tau}{2})}\, e^{-2\imath\pi f\tau} d\tau. \tag{47}$$

In Sections 5.4 (for Neumann's boundary condition) and 6.6 (for Robin's boundary condition), we will calculate an asymptotic expansion (when $f \to +\infty$) of the Wigner distribution of the random process $q$, which is such that $p(\boldsymbol{x}, t) = H(t)\, q(\boldsymbol{x}, t)$ as in (22) (the expressions of $q$ for the two boundary conditions were given in (23) and (37), respectively), rather than the Wigner distribution $W_p$ of the source response $p$, which is defined similarly to (46) and (45) by replacing $q$ with $p$. Indeed, $W_q$ admits a simpler closed-form expression, and is more meaningful, than $W_p$. Moreover, the Wigner distribution is a theoretical analysis tool, which in practice is approximated by another time-frequency distribution from Cohen's

[12]Non-mixing and non-ergodic billiards will be addressed in future publications (see Section 7).

class (Cohen, 1989) such as the spectrogram, which results in smoothing the Wigner distribution in the time-frequency plane[13]. However, the spectrogram of the source response at positive times can be equally obtained from the Wigner distribution of $p$, or that of $q$.

Anyway, note that the exact expression of $W_p$ can be easily derived from that of $W_q$, by applying the formula which expresses the Wigner distribution of a product, here $p(\boldsymbol{x}, t) = H(t)\, q(\boldsymbol{x}, t)$:

$$W_p(\boldsymbol{x}_1, \boldsymbol{x}_2, f, t) = \left( W_H(., t) \overset{f}{*} W_q(\boldsymbol{x}_1, \boldsymbol{x}_2, ., t) \right)(f), \tag{48}$$

where the Wigner distribution of the Heaviside function is obtained by applying (47) to $w(t) = H(t)$:

$$W_H(f, t) = 4t\,\mathrm{sinc}(4\pi f t) H(t). \tag{49}$$

*4.2. Assumption 1: Random source position*

The first assumption of the Statistical Wave Field Theory concerns the position of the source in the domain space $V$:

> **Assumption 1:** The punctual source's position is a random variable uniformly distributed in $V$.

As explained in the introduction, the randomized source position permits us to translate certain mathematical properties of dynamical billiards which are actually deterministic and related to chaos, into the more accessible language of the theory of probability. More precisely, the uniform distribution of the source's position $\boldsymbol{x}_0$ is in agreement with the ergodic property[14] introduced in Section 3.6.1. Moreover, Assumption 1 makes the statistics of the source response at any space position $\boldsymbol{x}$ independent of the actual source position, in agreement with the mixing property.

Assumption 1 implies that the values of the eigenfunctions at the source position also are random variables:

**Lemma 1** (White noise property)**.**

- *In the case of Neumann's boundary condition,* $\phi_0(\boldsymbol{x}_0) = \sqrt{\lambda}$*, and the real random sequence* $\{\phi_n(\boldsymbol{x}_0)\}_{n\in\mathbb{N}^*}$ *is white noise of variance* $\lambda = \frac{1}{|V|}$.

- *In the case of Robin's boundary condition, the complex random variables* $\varphi_n(\boldsymbol{x}_0, k)$ *are such that*

$$\forall n_1, n_2 \in \mathbb{N},\ \mathbb{E}\left[\varphi_{n_1}(\boldsymbol{x}_0, k)\varphi_{n_2}(\boldsymbol{x}_0, k)\right] = \lambda\, \delta_{n_1,n_2}. \tag{50}$$

[13]Indeed, the Wigner distribution has one main advantage, which is its high time-frequency resolution, but two serious drawbacks: it is non-local and prone to interference terms. On the contrary, the spectrogram, when computed with a window of bounded temporal support, is local over time and does not produce interference terms, at the cost of a degraded time-frequency resolution.

[14]Assuming that the orientation of the source is also uniformly distributed would not make sense here, since a punctual source response is isotropic (see equation (6)).

*Proof.* Let us first consider Neumann's boundary condition. We already know that $\phi_0(\boldsymbol{x}_0) = \sqrt{\lambda}$ (*cf.* Section 3.3.2). If we multiply both members of (19) with $\phi_n(\boldsymbol{y})$ and if we integrate over $\boldsymbol{y}$ in $V$, we get $\forall n_1, n_2 \in \mathbb{N}$, $\int_{\boldsymbol{x}\in V} \phi_{n_1}(\boldsymbol{x})\phi_{n_2}(\boldsymbol{x})d\boldsymbol{x} = \delta_{n_1,n_2}$. If we apply this equality to $n_2 = 0$ and $n_1 = n \neq 0$, we get $\mathbb{E}\left[\varphi_n(\boldsymbol{x}_0)\right] = 0$, so the random variables $\phi_n(\boldsymbol{x}_0)$ are centered for $n \in \mathbb{N}^*$. In addition, the same equation proves that $\mathbb{E}\left[\phi_{n_1}(\boldsymbol{x}_0)\phi_{n_2}(\boldsymbol{x}_0)\right] = \lambda\, \delta_{n_1,n_2}$. We conclude that the random variables $\phi_n(\boldsymbol{x}_0)$ are uncorrelated and of variance $\lambda$ for $n \in \mathbb{N}^*$.

Let us now consider Robin's boundary condition. If we multiply both members of (32) with $\varphi_n(\boldsymbol{y}, k)$ and if we integrate over $\boldsymbol{y}$ in $V$, we get $\forall n_1, n_2 \in \mathbb{N}$, $\int_{\boldsymbol{x}\in V} \varphi_{n_1}(\boldsymbol{x}, k)\varphi_{n_2}(\boldsymbol{x}, k)d\boldsymbol{x} = \delta_{n_1,n_2}$, which proves (50). □

Moreover, in the case of Neumann's boundary condition, remember that the expression of the source response $p(\boldsymbol{x}, \boldsymbol{x}_0, t)$ in (22) involves the random process $q(\boldsymbol{x}, \boldsymbol{x}_0, t)$ defined in (23). Then, by applying Lemma 1, we get from (23) the expected value of the random process $q$:

$$\mu_q(\boldsymbol{x}, t) \triangleq \mathbb{E}[q(\boldsymbol{x}, t)] = \lambda c^2,$$

which means that $q$ is first order stationary over both space and time, of mean $\lambda c^2$.

Regarding the ACF defined in (45), we get

$$\Gamma_q(\boldsymbol{x}_1, \boldsymbol{x}_2, t_1, t_2) = \tfrac{\lambda c^4}{2} \sum_{n\in\mathbb{N}^*} \phi_n(\boldsymbol{x}_1)\, \phi_n(\boldsymbol{x}_2) \left(\cos(2\pi c k_n(t_1 - t_2)) + \cos(2\pi c k_n(t_1 + t_2))\right). \quad (51)$$

If we now consider the Wigner distribution of $q$, by substituting (51) into (46), we get

$$\begin{aligned} W_q(\boldsymbol{x}_1, \boldsymbol{x}_2, f, t) = & \tfrac{\lambda c^4}{4} \sum_{n\in\mathbb{N}^*} \phi_n(\boldsymbol{x}_1)\, \phi_n(\boldsymbol{x}_2) \left(\delta(f - c k_n) + \delta(f + c k_n) + 2\delta(f) \cos(4\pi c k_n t)\right) \\ = & \tfrac{\lambda c^2}{2} \left(\widehat{q}(\boldsymbol{x}_1, \boldsymbol{x}_2, f) + \delta(f) \left(q(\boldsymbol{x}_1, \boldsymbol{x}_2, 2t) - 2\lambda c^2\right)\right). \end{aligned} \quad (52)$$

where $\widehat{q}(\boldsymbol{x}_1, \boldsymbol{x}_2, f)$ denotes the 1D Fourier transform (1) of $q(\boldsymbol{x}_1, \boldsymbol{x}_2, t)$ w.r.t. time.

When $f \neq 0$, equation (52) reduces to

$$W_q(\boldsymbol{x}_1, \boldsymbol{x}_2, f, t) = \tfrac{\lambda c^2}{2} \widehat{q}(\boldsymbol{x}_1, \boldsymbol{x}_2, f), \quad (53)$$

which is stationary over time. Therefore, if we omit the zero frequency, we conclude that $q$ is a WSS process over time. However, under the sole Assumption 1, it is not second order stationary over space, because the Wigner distribution $W_q$ in (53) is not a function of $\boldsymbol{x}_1 - \boldsymbol{x}_2$.

In Section 4.4, we will introduce the additional Assumption 3, that will permit us to define a stationary Wigner distribution by calculating stationary second order statistics of the $B$-function. Before doing that, we need to investigate here the consequences of the sole Assumption 1 on the statistics of the $B$-function.

#### *4.2.1. Neumann's boundary condition*

In the case of Neumann's boundary condition, the expression of the $B$-function was given in (24). Regarding its first order statistics, we have

$$\mu_B(\boldsymbol{y}) \triangleq \mathbb{E}[B(\boldsymbol{y}, \boldsymbol{x}_0)] = \lambda \int_{\boldsymbol{x}_0\in V} B(\boldsymbol{y}, \boldsymbol{x}_0) d\boldsymbol{x}_0. \quad (54)$$

Then, by substituting (24) into (54), Lemma 1 implies that

$$\mu_B(\boldsymbol{y}) = \lambda, \tag{55}$$

so the $B$-function is first-order stationary. Regarding the second order statistics, we have

$$\Gamma_B(\boldsymbol{y}_1, \boldsymbol{y}_2) = \operatorname{cov}[B(\boldsymbol{y}_1, \boldsymbol{x}_0), B(\boldsymbol{y}_2, \boldsymbol{x}_0)] = \lambda \int_{\boldsymbol{x}_0 \in V} B(\boldsymbol{y}_1, \boldsymbol{x}_0) B(\boldsymbol{y}_2, \boldsymbol{x}_0) d\boldsymbol{x}_0 - \lambda^2. \tag{56}$$

By substituting (24) into (56), Lemma 1 implies that

$$\Gamma_B(\boldsymbol{y}_1, \boldsymbol{y}_2) = \lambda \sum_{n \in \mathbb{N}^*} \phi_n(\boldsymbol{y}_1)\, \phi_n(\boldsymbol{y}_2) = \lambda B(\boldsymbol{y}_1, \boldsymbol{y}_2) - \lambda^2 \tag{57}$$

so the $B$-function is not second-order stationary ($\Gamma_B$ is not a function of $\boldsymbol{y}_1 - \boldsymbol{y}_2$).

*4.2.2. Robin's boundary condition*

In the case of Robin's boundary condition, the expression of the $B$-function was given in (38). Regarding its first order statistics, we have

$$\mu_B(\boldsymbol{y}, k) \triangleq \mathbb{E}[B(\boldsymbol{y}, \boldsymbol{x}_0, k)] = \lambda \int_{\boldsymbol{x}_0 \in V} B(\boldsymbol{y}, \boldsymbol{x}_0, k) d\boldsymbol{x}_0. \tag{58}$$

The mean $\mu_B(\boldsymbol{y}, k)$ can only be calculated in closed-form for $k = 0$, which corresponds to Neumann's boundary condition:

$$\mu_B(\boldsymbol{y}, 0) = \lambda, \tag{59}$$

so $B(\boldsymbol{y}, 0)$ is first-order stationary. However, for $k \neq 0$, the $B$-function is generally not first-order stationary ($\mu_B(\boldsymbol{y}, k)$ in (58) does depend on $\boldsymbol{y}$).

Regarding the second order statistics, as mentioned in Section 3.4.2, the eigenfunctions $\varphi_n$ are not orthogonal w.r.t. the Hermitian inner product when $k \neq 0$. For this reason, we cannot calculate in closed-form the covariances

$$\begin{aligned} \Gamma_B(\boldsymbol{y}_1, \boldsymbol{y}_2, k) = &\ \operatorname{cov}[B(\boldsymbol{y}_1, \boldsymbol{x}_0, k), B(\boldsymbol{y}_2, \boldsymbol{x}_0, k)] \\ = &\ \lambda \textstyle\int_{\boldsymbol{x}_0 \in V} B(\boldsymbol{y}_1, \boldsymbol{x}_0, k) \overline{B(\boldsymbol{y}_2, \boldsymbol{x}_0, k)} d\boldsymbol{x}_0 - |\mu_B(\boldsymbol{y}, k)|^2 \end{aligned}$$

of the complex random process $B$. However, the expression of its *pseudo-covariances* $J_B(\boldsymbol{y}_1, \boldsymbol{y}_2, k)$ can be simplified in the same way as the covariances in the case of Neumann's boundary condition in Section 4.2.1:

$$\begin{aligned} J_B(\boldsymbol{y}_1, \boldsymbol{y}_2, k) = &\ \operatorname{cov}[B(\boldsymbol{y}_1, \boldsymbol{x}_0, k), \overline{B(\boldsymbol{y}_2, \boldsymbol{x}_0, k)}] \\ = &\ \lambda \textstyle\int_{\boldsymbol{x}_0 \in V} B(\boldsymbol{y}_1, \boldsymbol{x}_0, k) B(\boldsymbol{y}_2, \boldsymbol{x}_0, k) d\boldsymbol{x}_0 - \mu_B(\boldsymbol{y}, k)^2. \end{aligned} \tag{60}$$

Indeed, by substituting (38) into (60), Lemma 1 shows that

$$J_B(\boldsymbol{y}_1, \boldsymbol{y}_2, k) = \lambda \sum_{n \in \mathbb{N}} \varphi_n(\boldsymbol{y}_1, k)\, \varphi_n(\boldsymbol{y}_2, k) - \mu_B(\boldsymbol{y}, k)^2 = \lambda B(\boldsymbol{y}_1, \boldsymbol{y}_2, k) - \mu_B(\boldsymbol{y}, k)^2, \tag{61}$$

which is similar to (57). Yet, the $B$-function is not pseudo-stationary ($J_B$ is not a function of $\boldsymbol{y}_1 - \boldsymbol{y}_2$).

*4.3. Assumption 2: High frequency*

As stated in Section 4.2, in the case of Neumann's boundary condition, if we omit the zero frequency, the random process $q(\boldsymbol{x}, \boldsymbol{x}_0, t)$ is WSS over time, of power spectrum $\widehat{\Gamma}_q(\boldsymbol{x}_1, \boldsymbol{x}_2, f) \triangleq \frac{\lambda c^2}{2} \widehat{q}(\boldsymbol{x}_1, \boldsymbol{x}_2, f)$ (see equation (53)). In order to further investigate the spectral properties of this WSS process, we need to introduce the second assumption:

| **Assumption 2:** The frequency $f$ (or equivalently the wave number $k$) is large. |
|---|

This assumption will permit us to consider only small delays $\tau = t_1 - t_2$ between times $t_1$ and $t_2$, and small distances $\|\boldsymbol{x}_1 - \boldsymbol{x}_2\|_2$ between two space positions $\boldsymbol{x}_1$ and $\boldsymbol{x}_2$, as explained in the following.

Remember that at high frequency, the density of modes increases quadratically, so the spectrum is better described by a smooth spectral density (see Section 3.5.1). However, we note that smoothing the discrete spectrum $\widehat{\Gamma}_q(\boldsymbol{x}_1, \boldsymbol{x}_2, f)$ over frequency $f$ is equivalent to smoothing the source frequency response $\widehat{q}(\boldsymbol{x}_1, \boldsymbol{x}_2, f)$ over $f$. This can be achieved by multiplying $q(\boldsymbol{x}_1, \boldsymbol{x}_2, \tau)$ with a window function $w_\varepsilon(\tau)$ of finite temporal support $]-\varepsilon, +\varepsilon[$ for a given $\varepsilon > 0$. Indeed, this multiplication in the time domain is equivalent to convoluting in the frequency domain $\widehat{q}(\boldsymbol{x}_1, \boldsymbol{x}_2, f)$ with the 1D-Fourier transform (1) of the window function $w_\varepsilon(\tau)$. Consequently, the smoothed spectrum is characterized by function $q(\boldsymbol{x}_1, \boldsymbol{x}_2, \tau)$ at times $|\tau| < \varepsilon$, or equivalently by the source response $p(\boldsymbol{x}_1, \boldsymbol{x}_2, |\tau|)$ at times $|\tau| < \varepsilon$. However, because $p$ is the causal solution to the inhomogeneous wave equation (5), $p$ is identically zero in the time interval $[0, \varepsilon[$ as soon as $\|\boldsymbol{x}_1 - \boldsymbol{x}_2\|_2 \geq c\,\varepsilon$. If on the contrary $\|\boldsymbol{x}_1 - \boldsymbol{x}_2\|_2 < c\,\varepsilon$, then the direct path $\frac{\dot{\delta}\left(\tau - \frac{\|\boldsymbol{x}_1 - \boldsymbol{x}_2\|_2}{c}\right)}{4\pi\|\boldsymbol{x}_1 - \boldsymbol{x}_2\|_2}$ between $\boldsymbol{x}_1$ and $\boldsymbol{x}_2$ (see equation (6)) falls in the time interval $[0, \varepsilon[$. If in addition $\boldsymbol{x}_1$ and $\boldsymbol{x}_2$ belong to a certain vicinity of the boundary of $V$, then the first reflection between $\boldsymbol{x}_1$ and $\boldsymbol{x}_2$ may also fall in the time interval $[0, \varepsilon[$.

To summarize, we can distinguish two cases when $\varepsilon \to 0$:

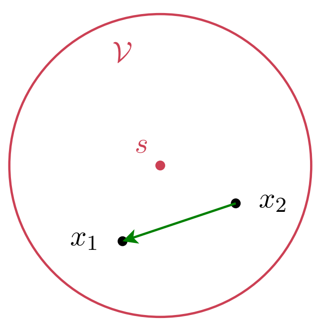


Figure 1: **Interior points**: the two space positions $\boldsymbol{x}_1$ and $\boldsymbol{x}_2$ belong to the same vicinity $\mathcal{V} \subset \mathring{V}$ (red circle) of an interior point $\boldsymbol{s} \in \mathring{V}$, so that the direct path from $\boldsymbol{x}_2$ to $\boldsymbol{x}_1$ (green arrow) is included in $\mathcal{V}$.

1. if both $\boldsymbol{x}_1$ and $\boldsymbol{x}_2$ belong to the vicinity $\mathcal{V} \subset \mathring{V}$ of an interior point $\boldsymbol{s} \in \mathring{V}$, then the windowed function $w_\varepsilon(\tau)\, q(\boldsymbol{x}_1, \boldsymbol{x}_2, \tau)$ includes only the direct path between $\boldsymbol{x}_1$ and $\boldsymbol{x}_2$.

This situation is illustrated in Figure 1: the vicinity of $\boldsymbol{s}$ (inside the red circle) is the open ball $\mathcal{V} = \mathcal{B}(\boldsymbol{s}, \frac{c\varepsilon}{2})$, which implies $\|\boldsymbol{x}_1 - \boldsymbol{x}_2\|_2 < c\,\varepsilon$, so that the direct path from $\boldsymbol{x}_2$ to $\boldsymbol{x}_1$ (green arrow) follows in the time interval $[0, \varepsilon[$.

2. if both $\boldsymbol{x}_1$ and $\boldsymbol{x}_2$ belong to the vicinity $\mathcal{V} \subset \overline{V}$ of a boundary point $\boldsymbol{s} \in \partial V$, then the windowed function $w_\varepsilon(\tau)\, q(\boldsymbol{x}_1, \boldsymbol{x}_2, \tau)$ includes both the direct path and the first reflection on the boundary near $\boldsymbol{s}$. This situation is illustrated in Figure 2: the domain's boundary is represented in blue, its tangent plane $T(\boldsymbol{s})$ and outward normal vector $\boldsymbol{n}(\boldsymbol{s})$ at $\boldsymbol{s}$ in black, and the exterior of the domain is hatched. The direct path and the first reflection are represented with green arrows. The image of $\boldsymbol{x}_2$ is $\boldsymbol{x}_2' = \boldsymbol{x}_2 - 2\boldsymbol{n}(\boldsymbol{s})\boldsymbol{n}(\boldsymbol{s})^\top(\boldsymbol{x}_2 - \boldsymbol{s})$.

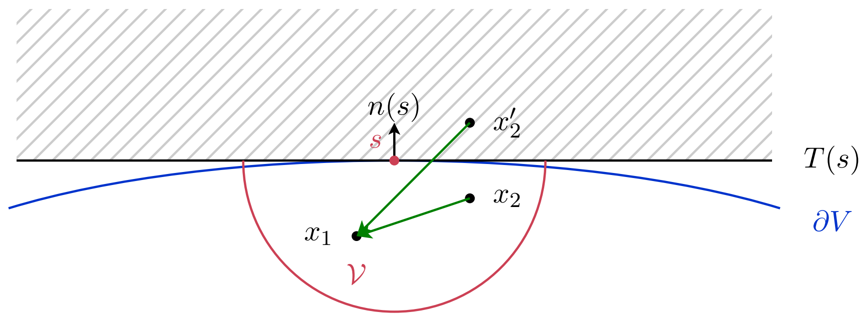


Figure 2: **Boundary points**: $\boldsymbol{s}$ now belongs to the boundary surface (blue curve), which is locally approximated be its tangent plane $T(\boldsymbol{s})$ (black line), that is orthogonal to the outward normal vector $\boldsymbol{n}(\boldsymbol{s})$. The two space positions $\boldsymbol{x}_1$ and $\boldsymbol{x}_2$ still belong to the same vicinity $\mathcal{V} \subset \mathring{V}$, which is now bounded by $T(\boldsymbol{s})$ and by the red semicircle. The image of $\boldsymbol{x}_2$, denoted $\boldsymbol{x}_2'$, lies in the exterior of the domain (hatched region). The direct path and first reflection are represented with green arrows.

Now let us focus again on the statistics of the $B$-function. In the two cases of Neumann and Robin's boundary conditions, the second order statistics $\Gamma_B(\boldsymbol{y}_1, \boldsymbol{y}_2)$ and $J_B(\boldsymbol{y}_1, \boldsymbol{y}_2, k)$ have been expressed in terms of the $B$-function itself in equations (57) and (61), respectively. Considering the previous discussion, we can distinguish the same two cases for $\boldsymbol{y} = \boldsymbol{y}_1$ and small values of $\boldsymbol{z} = \boldsymbol{y}_1 - \boldsymbol{y}_2$:

1. if $\boldsymbol{y}$ belongs to the vicinity $\mathcal{V} \subset \mathring{V}$ of an interior point $\boldsymbol{s} \in \mathring{V}$, then after spectral smoothing the term involving the $B$-function in (57) and (61) includes only the direct path: $B(\boldsymbol{y}_1, \boldsymbol{y}_2, k) = \delta(\boldsymbol{y}_1 - \boldsymbol{y}_2)$.
2. if $\boldsymbol{y}$ belongs to the vicinity $\mathcal{V} \subset \overline{V}$ of a boundary point $\boldsymbol{s} \in \partial V$, then after spectral smoothing the term involving the $B$-function in (57) and (61) includes both the direct path and the first reflection on the boundary near $\boldsymbol{s}$. Moreover, under the high frequency Assumption 2, $\partial V$ can be locally approximated by its tangent plane $T(\boldsymbol{s})$ represented in Figure 2, so that the two expressions of the $B$-function in (18) and (29), which we obtained in the case of a plane boundary, can be substituted into equations (57) and (61), respectively.

*4.4. Assumption 3: Stationarity of the B-function*

As briefly discussed in Section 3.6.1, in a mixing billiard, the statistics of the reflections are defined independently of the source position (which led us to Assumption 1), and they are also independent of the receiver position and orientation. In the formalism used in this paper, the reflections are implicitly described by the $B$-function, which defines the spatial distribution of the image sources, as explained in Section 3.2. So the mixing property can be reformulated in terms of the $B$-function as follows: the statistics of the $B$-function are independent of the spatial position and orientation, or more precisely:

| |
|---|
| **Assumption 3:** The mean and (pseudo-)covariances of the $B$-function are stationary and isotropic. |

This assumption will be formalized by averaging the first and second order statistics of the $B$-function that we calculated in Section 4.2 based on the sole Assumption 1 about the source position, so as to make them both stationary and isotropic. More precisely, we will calculate space-averaged statistics of the $B$-function, which will be obtained as sums of contributions coming from all points $\boldsymbol{s}$ in the domain $\overline{V}$. Indeed, we have seen in Section 4.3 that the smoothed spectrum of the source response is related to the local statistics of the $B$-function in the vicinity $\mathcal{V}$ of points $\boldsymbol{s}$ that may lie either in the interior $\mathring{V}$ or at the boundary $\partial V$. These local statistics will now be formally defined and averaged, in the two cases of Neumann's (Section 4.4.1) and Robin's (Section 4.4.2) boundary conditions.

*4.4.1. Neumann's boundary condition*

For a given vicinity $\mathcal{V}$ of a point $\boldsymbol{s}$ in $\overline{V}$, we introduce the WSS process $\xi(\boldsymbol{y}, \mathcal{V})$, whose statistics are defined as follows:

- The local mean $\mu_\xi(\mathcal{V})$ is defined as a weighted integral of $\mu_B(\boldsymbol{y})$ in (55) over $\mathcal{V}$:

$$\mu_\xi(\mathcal{V}) = \lambda \int_{\boldsymbol{y}\in\mathcal{V}} \mu_B(\boldsymbol{y})\, d\boldsymbol{y} = \lambda^2 |\mathcal{V}|. \tag{62}$$

- For a given vector $\boldsymbol{z}$ in a mathematical vicinity of $\mathbf{0}$ (which is such that $\boldsymbol{y} - \boldsymbol{z} \in \mathcal{D}$ $\forall \boldsymbol{y} \in \mathcal{V}$), the local stationary ACF $\Lambda^0(\boldsymbol{z}, \mathcal{V})$ is defined as a weighted integral over $\boldsymbol{y} \in \mathcal{V}$ of $\Gamma_B(\boldsymbol{y}, \boldsymbol{y} - \boldsymbol{z})$ in (57) (in order to enforce stationarity):

$$\begin{aligned} \Lambda^0(\boldsymbol{z}, \mathcal{V}) = & \ \lambda \textstyle\int_{\boldsymbol{y}\in\mathcal{V}} \Gamma_B(\boldsymbol{y}, \boldsymbol{y} - \boldsymbol{z})\, d\boldsymbol{y} \\ = & \ \lambda^2 \textstyle\int_{\boldsymbol{y}\in\mathcal{V}} B(\boldsymbol{y}, \boldsymbol{y} - \boldsymbol{z})\, d\boldsymbol{y} \end{aligned} \tag{63}$$

  where we have substituted (57), from which we have removed the constant term $\lambda^2$, since we are working under the high frequency Assumption 2.

- For a given wave number $k \in \mathbb{R}_+$, the local isotropic power spectrum $\widehat{\Lambda}^0(k, \mathcal{V})$ is defined as the integral over $\boldsymbol{k} \in \mathcal{S}(0, k)$ (in order to enforce isotropy) of the 3D Fourier transform (2) of $\Lambda^0(\boldsymbol{z}, \mathcal{V})$ in (63):

$$\widehat{\Lambda}^0(k, \mathcal{V}) = \int_{\boldsymbol{k}\in\mathcal{S}(0,k)} \widehat{\Lambda}^0(\boldsymbol{k}, \mathcal{V}) dS(\boldsymbol{k}). \tag{64}$$

Note that we consider in (64) the 3D Fourier transform $\widehat{\Lambda}^0(\boldsymbol{k},\mathcal{V})$ of the ACF $\Lambda^0(\boldsymbol{z},\mathcal{V})$, which implicitly involves an integral over $\boldsymbol{z}\in\mathbb{R}^3$, whereas $\Lambda^0(\boldsymbol{z},\mathcal{V})$ was actually defined for small values of $\boldsymbol{z}$ only in (63). Indeed, we will see in Section 5.1 that, in both cases of interior and boundary points $\boldsymbol{s}$, the closed-form expression of $\Lambda^0(\boldsymbol{z},\mathcal{V})$ that we will get from (63) naturally leads to a smooth power spectrum $\widehat{\Lambda}^0(k,\mathcal{V})$ in (64), so this smooth power spectrum will be defined independently of the window function $w_\varepsilon(\tau)$ which we introduced in Section 4.3 and which explicitly restricts $\boldsymbol{z}$ to small values.

When integrating over the whole domain, i.e. when $\mathcal{V}=\overline{V}$, the random process $\xi(\boldsymbol{y},\overline{V})$ is identified to the $B$-function $B(\boldsymbol{y})$, so we retrieve from (62) the mean value $\mu_B(\boldsymbol{y})=\mu_\xi(\overline{V})=\lambda$ (equation (55)) and we get from (64) the expression of the isotropic power spectrum of the $B$-function:

$$\widehat{\Gamma}_B(k)\triangleq\widehat{\Lambda}^0(k,\overline{V})=\int_{\boldsymbol{k}\in\mathcal{S}(0,k)}\widehat{\Lambda}^0(\boldsymbol{k},\overline{V})dS(\boldsymbol{k}). \tag{65}$$

*4.4.2. Robin's boundary condition*

In the case of Robin's boundary condition, we also want to introduce stationary statistics of the $B$-function, as we did in Section 4.4.1. However, contrary to the case of Neumann's boundary condition, we cannot assume that the covariances are stationary. Indeed, when there is absorption at the domain's boundary, the normal modes are exponentially decaying over time, so the source response is non-stationary over time (see equation (37)). Because it is a solution to the wave equation, it is therefore also non-stationary over space. So the power of the source response actually depends on the space position, thus the variance of the $B$-function also depends on the space position. Yet, the mixing property suggests a form of second order stationarity of the $B$-function, as in Section 4.4.1. Considering the formal similarity between equations (61) and (57), we will thus define an isotropic pseudo spectrum $\widehat{J}_B$, similarly to the isotropic power spectrum $\widehat{\Gamma}_B$ in equation (65). For a given vicinity $\mathcal{V}$ of a point $\boldsymbol{s}$ in $\overline{V}$, we introduce the complex random process $\zeta(\boldsymbol{y},\mathcal{V},k)$, whose statistics are defined as follows:

- The local mean $\mu_\zeta(\mathcal{V},k)$ is defined as a weighted integral of $\mu_B(\boldsymbol{y},k)$ in (58) over $\mathcal{V}$:

$$\mu_\zeta(\mathcal{V},k)=\lambda\int_{\boldsymbol{y}\in\mathcal{V}}\mu_B(\boldsymbol{y},k)d\boldsymbol{y}. \tag{66}$$

- For a given vector $\boldsymbol{z}$ in a mathematical vicinity of $\mathbf{0}$ (which is such that $\boldsymbol{y}-\boldsymbol{z}\in\mathcal{D}$ $\forall\boldsymbol{y}\in\mathcal{V}$), the local stationary *pseudo-covariance function* (PCF) $J_\zeta(\boldsymbol{z},\mathcal{V},k)$ is defined as a weighted integral over $\boldsymbol{y}\in\mathcal{V}$ of $J_B(\boldsymbol{y},\boldsymbol{y}-\boldsymbol{z},k)$ in (61) (in order to enforce stationarity):

$$\begin{aligned}J_\zeta(\boldsymbol{z},\mathcal{V},k)=&\ \lambda\textstyle\int_{\boldsymbol{y}\in\mathcal{V}}J_B(\boldsymbol{y},\boldsymbol{y}-\boldsymbol{z},k)\,d\boldsymbol{y}\\=&\ \lambda^2\textstyle\int_{\boldsymbol{y}\in\mathcal{V}}B(\boldsymbol{y},\boldsymbol{y}-\boldsymbol{z},k)\,d\boldsymbol{y}\end{aligned} \tag{67}$$

  where we have substituted (61), from which we have removed the mean term (which would have resulted in a constant term due to (69)), since we are working under the high frequency Assumption 2.

- For a given wave number $\kappa \in \mathbb{R}_+$, the local isotropic pseudo spectrum $\widehat{J}_\zeta(\kappa, \mathcal{V}, k)$ is defined as the integral over $\boldsymbol{\kappa} \in \mathcal{S}(0, \kappa)$ (in order to enforce isotropy) of the 3D Fourier transform (2) of $J_\zeta(\boldsymbol{z}, \mathcal{V}, k)$ in (67):

$$\widehat{J}_\zeta(\kappa, \mathcal{V}, k) = \int_{\boldsymbol{\kappa} \in \mathcal{S}(0,\kappa)} \widehat{J}_\zeta(\boldsymbol{\kappa}, \mathcal{V}, k) dS(\boldsymbol{\kappa}). \tag{68}$$

  As in Section 4.4.1, note that we consider in (68) the 3D Fourier transform $\widehat{J}_\zeta(\boldsymbol{\kappa}, \mathcal{V}, k)$ of the PCF $J_\zeta(\boldsymbol{z}, \mathcal{V}, k)$, which implicitly involves an integral over $\boldsymbol{z} \in \mathbb{R}^3$, whereas $J_\zeta(\boldsymbol{z}, \mathcal{V}, k)$ was actually defined for small values of $\boldsymbol{z}$ only in (67). Indeed, we will see in Section 6.1 that, in both cases of interior and boundary points $\boldsymbol{s}$, the closed-form expression of $J_\zeta(\boldsymbol{z}, \mathcal{V}, k)$ that we will get from (67) naturally leads to a smooth pseudo spectrum $\widehat{J}_\zeta(\kappa, \mathcal{V}, k)$ in (68), so this smooth pseudo spectrum will be defined independently of the window function $w_\varepsilon(\tau)$ which we introduced in Section 4.3 and which explicitly restricts $\boldsymbol{z}$ to small values.

When integrating over the whole domain, i.e. when $\mathcal{V} = \overline{V}$, the random process $\zeta(\boldsymbol{y}, \overline{V}, k)$ is identified to the $B$-function $B(\boldsymbol{y}, k)$, so by substituting (58) into (66), the mean of the $B$-function is

$$\begin{aligned} \mu_B(k) = \;& \mu_\zeta(\overline{V}, k) = \lambda^2 \int_{\boldsymbol{y} \in V} \int_{\boldsymbol{x}_0 \in V} B(\boldsymbol{y}, \boldsymbol{x}_0, k)\, d\boldsymbol{x}_0 d\boldsymbol{y} \\ = \;& \lambda^2 \int_{\boldsymbol{y} \in V} \int_{\boldsymbol{x}_0 \in V} \delta(\boldsymbol{y} - \boldsymbol{x}_0)\, d\boldsymbol{x}_0 d\boldsymbol{y} = \lambda^2 |V| = \lambda, \end{aligned} \tag{69}$$

which generalizes (59) to all $k \in \mathbb{R}$. We also get from (68) the expression of the isotropic pseudo spectrum of the $B$-function:

$$\widehat{J}_B(\kappa, k) \triangleq \widehat{J}_\zeta(\kappa, \overline{V}, k) = \int_{\boldsymbol{\kappa} \in \mathcal{S}(0,\kappa)} \widehat{J}_\zeta(\boldsymbol{\kappa}, \overline{V}, k) dS(\boldsymbol{\kappa}). \tag{70}$$

## 5. Special Theory (Neumann's boundary condition)

Let us start with the case of Neumann's boundary condition. According to Assumption 3 introduced in Section 4.4, the $B$-function is a 3D WSS process defined on $\mathbb{R}^3$. Its second order statistics are thus characterized by its power spectrum $\widehat{\Gamma}_B(\boldsymbol{k})$, which is a measure (see Proposition 8.2.I. in (Daley and Vere-Jones, 2003, Chapter 8)), defined on the wave vector space $\mathbb{R}^3$. It turns out that the asymptotic expansion of the smoothed power spectrum can be informally derived from the developments in Section 3 by using a few intuitive arguments. Indeed, before spectral smoothing, equation (24) shows that $B(\boldsymbol{y}, \boldsymbol{x}_0) = \sum_{n \in \mathbb{N}} B_n(\boldsymbol{y}, \boldsymbol{x}_0)$ with $B_n(\boldsymbol{y}, \boldsymbol{x}_0) = \phi_n(\boldsymbol{x}_0)\, \phi_n(\boldsymbol{y})$. Since every eigenfunction $\phi_n$ is a solution to the Helmholtz equation (4) with the eigenvalue $k_n$, then so is the ACF $\Gamma_n(\boldsymbol{z})$ of the WSS process $B_n$. Therefore its 3D-Fourier transform, i.e. the measure $\widehat{\Gamma}_n(\boldsymbol{k})$, is supported in $\mathcal{S}(0, k_n)$ [15]. In other respects, the eigenfunctions $\phi_n$ form a Hilbert basis of $L^2(V)$, so they are unitary.

[15]Since $\Gamma_n(\boldsymbol{z}) = \int_{\boldsymbol{k} \in \mathbb{R}^3} e^{2\imath\pi \boldsymbol{k}^\top \boldsymbol{z}} d\widehat{\Gamma}_n(\boldsymbol{k})$, the Helmholtz equation (4) applied to $\Gamma_n(\boldsymbol{z})$ yields $4\pi^2(k_n^2 - \|\boldsymbol{k}\|^2)\widehat{\Gamma}_n(\boldsymbol{k}) = 0$, therefore either $\boldsymbol{k} \in \mathcal{S}(0, k_n)$ or $\widehat{\Gamma}_n(\boldsymbol{k}) = 0$.

Therefore the average energy of each mode $B_n$ is $\lambda^2 \int_{\boldsymbol{x}_0\in V}\int_{\boldsymbol{y}\in V} B_n(\boldsymbol{y},\boldsymbol{x}_0)^2 d\boldsymbol{y}d\boldsymbol{x}_0 = \lambda^2$. We thus conclude that $\widehat{\Gamma}_B(k_n) \triangleq \int_{\mathcal{S}(0,k_n)} d\widehat{\Gamma}_n(\boldsymbol{k}) = \lambda^2$.

However, in Section 3.5.1, equation (39) shows that the modal density admits the following asymptotic expansion in the case of Neumann's boundary condition: $\rho(k,0) = 4\pi\left(|V|k^2 + \frac{S(\partial V)}{8}k\right)$. By spectral smoothing, we thus get the following asymptotic expansion of the power spectral density:

$$\widehat{\Gamma}_B(k) = \lambda^2\,\rho(k,0) = 4\pi\lambda\left(k^2 + \tfrac{\lambda S(\partial V)}{8}k\right). \tag{71}$$

This equation will be formally proved in Section 5.1.3 (see equation (80)).

Then we will be able to deduce the asymptotic expansion when $f \to +\infty$ of the Wigner distribution $W_q(\boldsymbol{x}_1,\boldsymbol{x}_2,f,t)$ defined in (46) of the random process $q$ between two points $\boldsymbol{x}_1$ and $\boldsymbol{x}_2$ (Section 5.4). We will show that it can be factorized as $W_q(\boldsymbol{x}_1,\boldsymbol{x}_2,f,t) = W_q(f)\,\gamma(\boldsymbol{x}_1,\boldsymbol{x}_2,f)$ (equation (90)) where $W_q(f) = \frac{c^3}{4}\widehat{\Gamma}_B(\frac{f}{c}) = \pi\lambda c\left(f^2 + \frac{\lambda c S(\partial V)}{8}f\right)$ (equation (91)) is the stationary Wigner distribution at any point $\boldsymbol{x}\in V$, and $\gamma(\boldsymbol{x}_1,\boldsymbol{x}_2,f)$ is the spectral correlation (44) presented in Section 3.6.4.

### *5.1. Asymptotic expansion of the power spectrum*

As explained in Section 4.3, we will now distinguish the two following cases for $\boldsymbol{y} = \boldsymbol{y}_1$ and small values of $\boldsymbol{z} = \boldsymbol{y}_1 - \boldsymbol{y}_2$:

- if $\boldsymbol{y}$ belongs to the vicinity $\mathcal{V}\subset\mathring{V}$ of an interior point $\boldsymbol{s}\in\mathring{V}$, then the local power spectrum $\widehat{\Lambda}^0(k,\mathcal{V})$ introduced in Section 4.4.1 is asymptotically dominated by the direct path between $\boldsymbol{y}_1$ and $\boldsymbol{y}_2$ (Section 5.1.1);
- if $\boldsymbol{y}$ belongs to the vicinity $\mathcal{V}\subset\overline{V}$ of a boundary point $\boldsymbol{s}\in\partial V$, then the local power spectrum $\widehat{\Lambda}^0(k,\mathcal{V})$ is asymptotically dominated by both the direct path and the first reflection on the boundary near $\boldsymbol{s}$ (Section 5.1.2).

**Important remark**: from now on and until the end of this paper, all the mathematical expressions will hold as asymptotic expansions when the frequency $f$ or the wave number, denoted either $k$ or $\kappa$, tends to infinity, as in Section 3.5.1. However, for simplicity of notation, the remainder of the expansion (such as $O(\frac{1}{k})$) will not be written explicitly. Nevertheless, the reader should keep in mind that even when we write the expression of a function of space, such as $\Lambda^0(\boldsymbol{z},\mathcal{V})$ in the following, without saying it, we imply that this expression holds at high frequency, i.e. that the resulting expression of its 3D Fourier transform (2), denoted $\widehat{\Lambda}^0(\boldsymbol{k},\mathcal{V})$, holds asymptotically when $\|\boldsymbol{k}\|_2 \to +\infty$.

#### *5.1.1. Interior points*

In a vicinity $\mathcal{V}\subset\mathring{V}$ of a point $\boldsymbol{s}\in\mathring{V}$, we have

$$B(\boldsymbol{y}_1,\boldsymbol{y}_2) = \delta(\boldsymbol{y}_1 - \boldsymbol{y}_2) \tag{72}$$

(see Figure 1 in Section 4.3). Substituting this equation into (63), we get: $\Lambda^0(\boldsymbol{z},\mathcal{V}) = \lambda^2|\mathcal{V}|\,\delta(\boldsymbol{z})$, whose 3D Fourier transform (2) is $\widehat{\Lambda}^0(\boldsymbol{k},\mathcal{V}) = \lambda^2|\mathcal{V}|$. So by integrating $\widehat{\Lambda}^0(\boldsymbol{k},\mathcal{V})$ over the sphere $\mathcal{S}(0,k)$, we get the expression of $\widehat{\Lambda}^0(k,\mathcal{V})$ defined in (64):

$$\widehat{\Lambda}^0(k,\mathcal{V}) = 4\pi\lambda^2|\mathcal{V}|k^2. \tag{73}$$

Then, based on (62) and (73), the spectral representation theorem (see Theorem 8.4.IV in (Daley and Vere-Jones, 2003, Chapter 8)) shows that the WSS process $\xi(\boldsymbol{y},\mathcal{V})$ can be represented as[16]

$$\xi(\boldsymbol{y},\mathcal{V}) = \lambda^2|\mathcal{V}| + \int_{\boldsymbol{k}\in\mathbb{R}^3} e^{2\imath\pi\boldsymbol{k}^\top(\boldsymbol{y}-\boldsymbol{s})} d\widehat{\xi}^0(\boldsymbol{k},\mathcal{V}) \tag{74}$$

where $\boldsymbol{k}\mapsto\widehat{\xi}^0(\boldsymbol{k},\mathcal{V})$ is a centered complex random measure with uncorrelated increments on $\mathbb{R}^3$, which is Hermitian symmetric w.r.t. $\boldsymbol{k}$, such that for any Borel set $\mathcal{K}\subset\mathbb{R}^3$,

$$\mathbb{E}\left[\left(\widehat{\xi}^0(\mathcal{K},\mathcal{V})\right)^2\right] = 0 \quad\text{and}\quad \mathbb{E}\left[\left|\widehat{\xi}^0(\mathcal{K},\mathcal{V})\right|^2\right] = \int_{k\in\mathbb{R}_+} \tfrac{S(\mathcal{K}\cap\mathcal{S}(0,k))}{S(\mathcal{S}(0,k))}\,\widehat{\Lambda}^0(k,\mathcal{V})\,dk \tag{75}$$

with $\widehat{\Lambda}^0(k,\mathcal{V})$ the nonnegative spectral measure on $\mathbb{R}_+\times\mathring{V}$ expressed in (73).

*5.1.2. Boundary points*

As done in (Balian and Bloch, 1970, Section III-A), we will now use the *plane approximation*: the boundary surface in the vicinity $\mathcal{V}\subset\overline{V}$ of point $\boldsymbol{s}\in\partial V$, i.e. $\mathcal{V}\cap\partial V$, will be approximated by $\mathcal{V}\cap T(\boldsymbol{s})$, where $T(\boldsymbol{s})$ is the plane tangent to $\partial V$ at $\boldsymbol{s}$ (see Figure 2 in Section 4.3). So in a vicinity $\mathcal{V}\subset\overline{V}$ of $\boldsymbol{s}\in\partial V$, equation (18) shows that

$$B(\boldsymbol{y}_1,\boldsymbol{y}_2) = \delta(\boldsymbol{y}_1-\boldsymbol{y}_2) + \delta(\boldsymbol{y}_1-\boldsymbol{y}_2+2\boldsymbol{n}(\boldsymbol{s})\boldsymbol{n}(\boldsymbol{s})^\top(\boldsymbol{y}_2-\boldsymbol{s})) \tag{76}$$

where $\boldsymbol{y}_2 - 2\boldsymbol{n}(\boldsymbol{s})\boldsymbol{n}(\boldsymbol{s})^\top(\boldsymbol{y}_2-\boldsymbol{s})$ is the image of $\boldsymbol{y}_2$ by the reflection symmetry through plane $T(\boldsymbol{s})$. Then by substituting (76) into (63), we get

$$\begin{aligned}\Lambda^0(\boldsymbol{z},\mathcal{V}) =&\ \lambda^2\textstyle\int_{\boldsymbol{y}\in\mathcal{V}}\delta(\boldsymbol{z})+\delta(\boldsymbol{z}+2\boldsymbol{n}(\boldsymbol{s})\boldsymbol{n}(\boldsymbol{s})^\top(\boldsymbol{y}-\boldsymbol{z}-\boldsymbol{s}))\,d\boldsymbol{y}\\ =&\ \lambda^2\left(|\mathcal{V}|\delta(\boldsymbol{z})+\tfrac{1}{2}\delta(\boldsymbol{P}_{T(\boldsymbol{s})}^\top\boldsymbol{z})\textstyle\int_{\boldsymbol{y}\in\mathcal{V}}\delta(\boldsymbol{n}(\boldsymbol{s})^\top(\boldsymbol{y}-\boldsymbol{s}-\tfrac{\boldsymbol{z}}{2}))\,d\boldsymbol{y}\right)\\ =&\ \lambda^2\left(|\mathcal{V}|\delta(\boldsymbol{z})+\tfrac{S(\mathcal{V}\cap T(\boldsymbol{s}))}{2}\delta(\boldsymbol{P}_{T(\boldsymbol{s})}^\top\boldsymbol{z})H(-\boldsymbol{n}(\boldsymbol{s})^\top\boldsymbol{z})\right),\end{aligned}$$

which holds asymptotically when $\boldsymbol{z}\to\boldsymbol{0}$, and where $\boldsymbol{P}_{T(\boldsymbol{s})}$ denotes any $3\times 2$ orthonormal matrix whose range space is parallel to plane $T(\boldsymbol{s})$. Its 3D Fourier transform (2) is

$$\widehat{\Lambda}^0(\boldsymbol{k},\mathcal{V}) = \lambda^2\left(|\mathcal{V}|+\tfrac{S(\mathcal{V}\cap T(\boldsymbol{s}))}{4}\left(\tfrac{-1}{\imath\pi\boldsymbol{n}(\boldsymbol{s})^\top\boldsymbol{k}}+\delta(\boldsymbol{n}(\boldsymbol{s})^\top\boldsymbol{k})\right)\right).$$

So by integrating $\widehat{\Lambda}^0(\boldsymbol{k},\mathcal{V})$ over the sphere $\mathcal{S}(0,k)$, we get the expression of $\widehat{\Lambda}^0(k,\mathcal{V})$ defined in (64):

$$\widehat{\Lambda}^0(k,\mathcal{V}) = 4\pi\lambda^2\left(|\mathcal{V}|k^2+\tfrac{S(\mathcal{V}\cap T(\boldsymbol{s}))}{8}k\right), \tag{77}$$

[16] Note that vector $\boldsymbol{s}$ is subtracted to $\boldsymbol{y}$ in (74), because $\boldsymbol{s}$ is locally the origin of space in $\mathcal{V}$.

where we have used the fact that the circumference of the circle $\mathcal{S}(0,k)\cap \boldsymbol{n}(\boldsymbol{s})^\perp$ is $2\pi k$.

Then, based on (62) and (77), the spectral representation theorem shows that the WSS process $\xi(\boldsymbol{y},\mathcal{V})$ can be represented as in (74), where $\boldsymbol{k}\mapsto \widehat{\xi}^0(\boldsymbol{k},\mathcal{V})$ is still a centered complex random measure with uncorrelated increments on $\mathbb{R}^3$, which is Hermitian symmetric w.r.t. $\boldsymbol{k}$, such that for any Borel set $\mathcal{K}\subset\mathbb{R}^3$, equation (75) holds with $\widehat{\Lambda}^0(k,\mathcal{V})$ the nonnegative spectral measure on $\mathbb{R}_+\times\overline{V}$ expressed in (77).

### 5.1.3. Integrated power spectrum

If we assume that the random processes $\xi(\boldsymbol{y},\mathcal{V}_1)$ and $\xi(\boldsymbol{y},\mathcal{V}_2)$ are uncorrelated as soon as $\mathcal{V}_1\cap\mathcal{V}_2=\emptyset$, then by integrating over all points $\boldsymbol{s}\in\overline{V}$, we get from (73), (74), and (77) the following spectral representation of the resulting WSS random process $B(\boldsymbol{y})$:

$$B(\boldsymbol{y}) = \lambda + \int_{\boldsymbol{k}\in\mathbb{R}^3}\int_{\boldsymbol{s}\in\overline{V}} e^{2\imath\pi\boldsymbol{k}^\top(\boldsymbol{y}-\boldsymbol{s})} d\widehat{\xi}^0(\boldsymbol{k},\boldsymbol{s}) \tag{78}$$

where $\widehat{\xi}^0(\boldsymbol{k},\boldsymbol{s})$ is a centered complex random measure with uncorrelated increments on $\mathbb{R}^3\times\overline{V}$, which is Hermitian symmetric w.r.t. $\boldsymbol{k}$, such that for any Borel sets $\mathcal{K}\subset\mathbb{R}^3$ and $\mathcal{V}\subset\overline{V}$, equation (75) holds with $\widehat{\Lambda}^0(k,\mathcal{V})$ the nonnegative spectral measure on $\mathbb{R}_+\times\overline{V}$ defined as

$$\widehat{\Lambda}^0(k,\mathcal{V}) = 4\pi\lambda^2\left(|\mathcal{V}|k^2 + \tfrac{S(\mathcal{V}\cap\partial V)}{8}k\right), \tag{79}$$

where $S(\mathcal{V}\cap\partial V)$ replaces $S(\mathcal{V}\cap T(\boldsymbol{s}))$ in (77).

Hence the $B$-function is a WSS random process of mean $\mu_B=\lambda$, whose power spectrum $\widehat{\Gamma}_B(k)$ is obtained by substituting (79) into (65):

$$\widehat{\Gamma}_B(k) = \widehat{\Lambda}^0(k,\overline{V}) = 4\pi\lambda\left(k^2 + \tfrac{\lambda S(\partial V)}{8}k\right). \tag{80}$$

### 5.2. Green's function

Substituting (12) and (78) into (14) leads to the following spectral representation of the Green's function:

$$G(\boldsymbol{x},k) = \mu_G(k) + \int_{\boldsymbol{k}\in\mathbb{R}^3}\int_{\boldsymbol{s}\in\overline{V}} \frac{e^{2\imath\pi\boldsymbol{k}^\top(\boldsymbol{x}-\boldsymbol{s})}}{4\pi^2(\|\boldsymbol{k}\|_2^2-k^2)} d\widehat{\xi}^0(\boldsymbol{k},\boldsymbol{s}) \tag{81}$$

with

$$\mu_G(k) = \lambda\,\widehat{G}_0(\boldsymbol{0},k) = -\frac{\lambda}{4\pi^2k^2}. \tag{82}$$

### 5.3. Source response

Substituting (81) into (8) leads to

$$\dot{g}(\boldsymbol{x},t) = \mu_{\dot{g}}(t) - c^2\int_{\boldsymbol{k}\in\mathbb{R}^3}\int_{\boldsymbol{s}\in\overline{V}}\left(\int_{f\in\mathbb{R}} \frac{2\imath\pi f\, e^{2\imath\pi\boldsymbol{k}^\top(\boldsymbol{x}-\boldsymbol{s})}}{4\pi^2(f^2-c^2\|\boldsymbol{k}\|_2^2)}\, e^{2\imath\pi ft}df\right) d\widehat{\xi}^0(\boldsymbol{k},\boldsymbol{s}), \tag{83}$$

where (82) implies

$$\mu_{\dot{g}}(t) = \int_{f\in\mathbb{R}} \mu_G(\tfrac{f}{c})\, 2\imath\pi f\, e^{2\imath\pi f t} df = \tfrac{\lambda c^2}{2}\mathrm{sign}(t). \tag{84}$$

We note that the integrand in the integral over $f$ in (83) has two real poles, one at $f = c\|\boldsymbol{k}\|_2$ and one at $f = -c\|\boldsymbol{k}\|_2$. By applying the residue theorem to (83), we get a simplified expression of $\dot{g}(\boldsymbol{x}, t)$:

$$\dot{g}(\boldsymbol{x}, t) = \mu_{\dot{g}}(t) + \frac{c^2}{2}\mathrm{sign}(t) \int_{\boldsymbol{k}\in\mathbb{R}^3} \cos(2\pi c\|\boldsymbol{k}\|_2 t) \int_{\boldsymbol{s}\in\overline{V}} e^{2\imath\pi \boldsymbol{k}^\top(\boldsymbol{x}-\boldsymbol{s})} d\widehat{\xi}^0(\boldsymbol{k}, \boldsymbol{s}). \tag{85}$$

Substituting (85) into (11) leads to the same factorization of the source response as in (22):

$$p(\boldsymbol{x}, t) = H(t)\, q(\boldsymbol{x}, t) \tag{86}$$

where the random process $q(\boldsymbol{x}, t)$ admits the following spectral representation:

$$q(\boldsymbol{x}, t) = c^2 \left(\lambda + \int_{\boldsymbol{k}\in\mathbb{R}^3} \cos(2\pi c\|\boldsymbol{k}\|_2 t) \int_{\boldsymbol{s}\in\overline{V}} e^{2\imath\pi \boldsymbol{k}^\top(\boldsymbol{x}-\boldsymbol{s})} d\widehat{\xi}^0(\boldsymbol{k}, \boldsymbol{s})\right) \tag{87}$$

which is to be compared to (23).

Based on (87), the ACF of $q$ defined in (45) is a tempered distribution, so that $\forall \psi(f) \in \mathcal{S}(\mathbb{R})$ such that $\psi(0) = 0$ at $f = 0$ (remember that we are working under the high frequency Assumption 2),

$$\left\langle \Gamma_q(\boldsymbol{x}_1, \boldsymbol{x}_2, t + \tfrac{\tau}{2}, t - \tfrac{\tau}{2}) \middle| \widehat{\psi}(\tau) \right\rangle = \tfrac{c^4}{4} \int_{k\in\mathbb{R}_+} \mathrm{sinc}(2\pi k\|\boldsymbol{x}_1 - \boldsymbol{x}_2\|_2)\, (\psi(ck) + \psi(-ck))\, \widehat{\Gamma}_B(k) dk \tag{88}$$

where the power spectrum $\widehat{\Gamma}_B(k)$ was expressed in (80).

*5.4. Wigner distribution*

By substituting (88) into (46), we get the asymptotic expression of the Wigner distribution of the random process $q$, which holds when $f \to +\infty$:

$$W_q(\boldsymbol{x}_1, \boldsymbol{x}_2, f, t) = \tfrac{c^3}{4}\, \mathrm{sinc}(2\pi \tfrac{f}{c}\|\boldsymbol{x}_1 - \boldsymbol{x}_2\|_2)\, \widehat{\Gamma}_B(\tfrac{f}{c}). \tag{89}$$

Then by substituting (80) into (89), we get

$$W_q(\boldsymbol{x}_1, \boldsymbol{x}_2, f, t) = W_q(f)\, \gamma(\boldsymbol{x}_1, \boldsymbol{x}_2, f) \tag{90}$$

where

$$W_q(f) \triangleq W_q(\boldsymbol{x}, \boldsymbol{x}, f, t) = \pi\lambda c \left(f^2 + \tfrac{\lambda c S(\partial V)}{8} f\right) \tag{91}$$

is the stationary Wigner distribution at any point $\boldsymbol{x} \in V$, and $\gamma(\boldsymbol{x}_1, \boldsymbol{x}_2, f)$ is the spectral correlation defined in equation (44).

## 6. General Theory (Robin's boundary condition)

Let us now move on to Robin's boundary condition. Our main purpose will be to prove that the specific admittance $\widehat{\beta}$ induces a non-linear distortion of the wave numbers:

$$\kappa(k) = k + \tfrac{\imath\lambda}{8\pi}\int_{\boldsymbol{s}\in\partial V}\left(\ln\left(\tfrac{1+\widehat{\beta}(\boldsymbol{s},k)}{1-\widehat{\beta}(\boldsymbol{s},k)}\right) - \widehat{\beta}(\boldsymbol{s},k)^2\ln\left(\tfrac{\widehat{\beta}(\boldsymbol{s},k)+1}{\widehat{\beta}(\boldsymbol{s},k)-1}\right) + 2\widehat{\beta}(\boldsymbol{s},k)\right)dS(\boldsymbol{s})$$

(see equation (117)) and we will show that this equation is related to Sabine's and Eyring's formulas presented in Section 3.6.2.

Then we will be able to deduce the closed-form expression of the Wigner distribution $W_q(\boldsymbol{x}_1,\boldsymbol{x}_2,f,t)$ of the random process $q$ between two points $\boldsymbol{x}_1$ and $\boldsymbol{x}_2$ (Section 6.6). We will show that it can be factorized as in Polack's formula (43):

$$W_q(\boldsymbol{x}_1,\boldsymbol{x}_2,f,t) = W_q(\boldsymbol{x}_1,\boldsymbol{x}_2,f)\, e^{-2\alpha(\frac{f}{c})t}$$

(see equation (122)) where $\alpha(k)$ is the spectral attenuation, and $W_q(\boldsymbol{x}_1,\boldsymbol{x}_2,f)$ involves a term (115) that generalizes the spectral correlation (44) in Section 3.6.4.

### *6.1. Asymptotic expansion of the pseudo spectrum*

As explained in Section 4.3, we will now distinguish the two following cases for $\boldsymbol{y} = \boldsymbol{y}_1$ and small values of $\boldsymbol{z} = \boldsymbol{y}_1 - \boldsymbol{y}_2$:

- if $\boldsymbol{y}$ belongs to the vicinity $\mathcal{V} \subset \mathring{V}$ of an interior point $\boldsymbol{s} \in \mathring{V}$, then the pseudo spectrum $\widehat{J}_\zeta$ introduced in Section 4.4.2 is asymptotically dominated by the direct path between $\boldsymbol{y}_1$ and $\boldsymbol{y}_2$ (Section 6.1.1);
- if $\boldsymbol{y}$ belongs to the vicinity $\mathcal{V} \subset \overline{V}$ of a boundary point $\boldsymbol{s} \in \partial V$, then the pseudo spectrum $\widehat{J}_\zeta$ is asymptotically dominated by both the direct path and the first reflection on the boundary near $\boldsymbol{s}$ (Section 6.1.2).

#### *6.1.1. Interior points*

In a vicinity $\mathcal{V} \subset \mathring{V}$ of a point $\boldsymbol{s} \in \mathring{V}$, the $B$-function is as in (72). By substituting (72) into (67), we get $J_\zeta(\boldsymbol{z},\mathcal{V},k) = \lambda^2|\mathcal{V}|\,\delta(\boldsymbol{z})$, whose 3D Fourier transform (2) is $\widehat{J}_\zeta(\boldsymbol{\kappa},\mathcal{V},k) = \lambda^2|\mathcal{V}|$. So by integrating $\widehat{J}_\zeta(\boldsymbol{\kappa},\mathcal{V},k)$ over the sphere $\mathcal{S}(0,\kappa)$, we get the expression of $\widehat{J}_\zeta(\kappa,\mathcal{V},k)$ defined in (68):

$$\widehat{J}_\zeta(\kappa,\mathcal{V},k) = 4\pi\lambda^2|\mathcal{V}|\kappa^2. \tag{92}$$

#### *6.1.2. Boundary points*

As in Section 5.1.2, we will now use the *plane approximation*: the boundary surface in the vicinity $\mathcal{V} \subset \overline{V}$ of point $\boldsymbol{s} \in \partial V$, i.e. $\mathcal{V} \cap \partial V$, will be approximated by $\mathcal{V} \cap T(\boldsymbol{s})$, where $T(\boldsymbol{s})$ is the plane tangent to $\partial V$ at $\boldsymbol{s}$ (see Figure 2 in Section 4.3). So in a vicinity $\mathcal{V} \subset \overline{V}$ of $\boldsymbol{s} \in \partial V$, if $\mathrm{Im}(\widehat{\beta}(\boldsymbol{s},k)) < 0$, equation (29) shows that

$$\begin{aligned}&B(\boldsymbol{y}_1,\boldsymbol{y}_2,k) = \delta(\boldsymbol{y}_1-\boldsymbol{y}_2) + \delta(\boldsymbol{y}_1-\boldsymbol{y}_2+2\boldsymbol{n}(\boldsymbol{s})\boldsymbol{n}(\boldsymbol{s})^\top(\boldsymbol{y}_2-\boldsymbol{s}))\\&-4\imath\pi k\widehat{\beta}(\boldsymbol{s},k)H(\boldsymbol{n}(\boldsymbol{s})^\top(\boldsymbol{y}_1+\boldsymbol{y}_2-2\boldsymbol{s}))e^{-2\imath\pi k\widehat{\beta}(\boldsymbol{s},k)\boldsymbol{n}(\boldsymbol{s})^\top(\boldsymbol{y}_1+\boldsymbol{y}_2-2\boldsymbol{s})}\delta(\boldsymbol{P}_{T(\boldsymbol{s})}^\top(\boldsymbol{y}_1-\boldsymbol{y}_2))\end{aligned} \tag{93}$$

where the local origin of space $\boldsymbol{s} \in \mathcal{V}$ has been subtracted to both vectors $\boldsymbol{y}_1$ and $\boldsymbol{y}_2$.

By substituting (93) into (67), we get

$$
\begin{aligned}
J_\zeta(\boldsymbol{z}, \mathcal{V}, k) = \ & \lambda^2 \int_{\boldsymbol{y}\in\mathcal{V}} \delta(\boldsymbol{z}) + \delta(\boldsymbol{z} + 2\boldsymbol{n}(\boldsymbol{s})\boldsymbol{n}(\boldsymbol{s})^\top(\boldsymbol{y} - \boldsymbol{z} - \boldsymbol{s})) \\
& -4\imath\pi k\widehat{\beta}(\boldsymbol{s}, k) H(\boldsymbol{n}(\boldsymbol{s})^\top(2\boldsymbol{y} - \boldsymbol{z} - 2\boldsymbol{s}))e^{-2\imath\pi k\widehat{\beta}(\boldsymbol{s},k)\boldsymbol{n}(\boldsymbol{s})^\top(2\boldsymbol{y}-\boldsymbol{z}-2\boldsymbol{s})}\delta(\boldsymbol{P}_{T(\boldsymbol{s})}^\top \boldsymbol{z})\, d\boldsymbol{y} \\
= \ & \lambda^2 \Big( |\mathcal{V}|\delta(\boldsymbol{z}) + \delta(\boldsymbol{P}_{T(\boldsymbol{s})}^\top \boldsymbol{z}) \int_{\boldsymbol{y}\in\mathcal{V}} \tfrac{1}{2}\delta(\boldsymbol{n}(\boldsymbol{s})^\top(\boldsymbol{y} - \boldsymbol{s} - \tfrac{\boldsymbol{z}}{2})) \\
& -4\imath\pi k\widehat{\beta}(\boldsymbol{s}, k) H(\boldsymbol{n}(\boldsymbol{s})^\top(\boldsymbol{y} - \boldsymbol{s} - \tfrac{\boldsymbol{z}}{2}))e^{-4\imath\pi k\widehat{\beta}(\boldsymbol{s},k)\boldsymbol{n}(\boldsymbol{s})^\top(\boldsymbol{y}-\boldsymbol{s}-\frac{\boldsymbol{z}}{2})}\, d\boldsymbol{y} \Big) \\
= \ & \lambda^2 \Big( |\mathcal{V}|\delta(\boldsymbol{z}) + S(\mathcal{V} \cap T(\boldsymbol{s}))\delta(\boldsymbol{P}_{T(\boldsymbol{s})}^\top \boldsymbol{z}) H(-\boldsymbol{n}(\boldsymbol{s})^\top \boldsymbol{z}) \\
& \left( \tfrac{1}{2} - 4\imath\pi k\widehat{\beta}(\boldsymbol{s}, k) \int_{u=\frac{\boldsymbol{n}(\boldsymbol{s})^\top \boldsymbol{z}}{2}}^{0} e^{-4\imath\pi k\widehat{\beta}(\boldsymbol{s},k)\left(u - \frac{\boldsymbol{n}(\boldsymbol{s})^\top \boldsymbol{z}}{2}\right)} du \right) \Big) \\
= \ & \lambda^2 \left( |\mathcal{V}|\delta(\boldsymbol{z}) + S(\mathcal{V} \cap T(\boldsymbol{s}))\delta(\boldsymbol{P}_{T(\boldsymbol{s})}^\top \boldsymbol{z}) H(-\boldsymbol{n}(\boldsymbol{s})^\top \boldsymbol{z}) \left( -\tfrac{1}{2} + e^{2\imath\pi k\widehat{\beta}(\boldsymbol{s},k)\boldsymbol{n}(\boldsymbol{s})^\top \boldsymbol{z}} \right) \right)
\end{aligned}
$$

which holds asymptotically when $\boldsymbol{z} \to \boldsymbol{0}$, where $\boldsymbol{P}_{T(\boldsymbol{s})}$ denotes any $3 \times 2$ orthonormal matrix whose range space is parallel to plane $T(\boldsymbol{s})$, and where we have introduced the change of variable $u = \boldsymbol{n}(\boldsymbol{s})^\top(\boldsymbol{y} - \boldsymbol{s})$. Its 3D Fourier transform (2) is

$$
\widehat{J}_\zeta(\boldsymbol{\kappa}, \mathcal{V}, k) = \lambda^2 \left( |\mathcal{V}| + \tfrac{S(\mathcal{V}\cap T(\boldsymbol{s}))}{4\pi} \left( \tfrac{1}{\imath \boldsymbol{n}(\boldsymbol{s})^\top \boldsymbol{\kappa}} - \pi\delta(\boldsymbol{n}(\boldsymbol{s})^\top \boldsymbol{\kappa}) + \tfrac{2\imath}{\boldsymbol{n}(\boldsymbol{s})^\top \boldsymbol{\kappa} - k\widehat{\beta}(\boldsymbol{s},k)} \right) \right). \qquad (94)
$$

Then the expression of $\widehat{J}_\zeta(\kappa, \mathcal{V}, k)$ defined in (68) is obtained by integrating $\widehat{J}_\zeta(\boldsymbol{\kappa}, \mathcal{V}, k)$ over the sphere $\mathcal{S}(0, \kappa)$. Considering the last term in (94), we first note that

$$
\frac{1}{2\pi} \int_{\boldsymbol{\kappa}\in\mathcal{S}(0,\kappa)} \frac{1}{\boldsymbol{n}(\boldsymbol{s})^\top \boldsymbol{\kappa} - k\widehat{\beta}(\boldsymbol{s},k)} dS(0, \kappa) = \kappa^2 \int_{u=-1}^{1} \frac{1}{\kappa u - k\widehat{\beta}(\boldsymbol{s},k)} du = \kappa \left( \ln\left( \frac{\kappa - k\widehat{\beta}(\boldsymbol{s},k)}{\kappa + k\widehat{\beta}(\boldsymbol{s},k)} \right) - \imath\pi \right) \qquad (95)
$$

where ln(.) denotes the principal branch of the complex logarithm, to which the term $\imath\pi$ is subtracted rather than added, because the sign of the imaginary part of the left member of (95) is negative, since we assumed that $\mathrm{Im}(\widehat{\beta}(\boldsymbol{s}, k)) < 0$, whereas the sign of the imaginary part of the logarithm in the right member is positive, for the same reason.

By substituting equations (94) and (95) into (68), we get

$$
\begin{aligned}
\widehat{J}_\zeta(\kappa, \mathcal{V}, k) = \ & 4\pi\lambda^2 \left( |\mathcal{V}|\kappa^2 + \tfrac{S(\mathcal{V}\cap T(\boldsymbol{s}))}{4\pi} \int_{\boldsymbol{\kappa}\in\mathcal{S}(0,\kappa)} \left( -\tfrac{\delta(\boldsymbol{n}(\boldsymbol{s})^\top \boldsymbol{\kappa})}{4} + \imath \tfrac{1}{2\pi} \tfrac{1}{\boldsymbol{n}(\boldsymbol{s})^\top \boldsymbol{\kappa} - k\widehat{\beta}(\boldsymbol{s},k)} \right) \right) dS(\boldsymbol{\kappa}) \\
= \ & 4\pi\lambda^2 \left( |\mathcal{V}|\kappa^2 + \tfrac{S(\mathcal{V}\cap T(\boldsymbol{s}))}{4\pi} \left( -\tfrac{\pi\kappa}{2} + \imath\kappa \left( \ln\left( \tfrac{\kappa - k\widehat{\beta}(\boldsymbol{s},k)}{\kappa + k\widehat{\beta}(\boldsymbol{s},k)} \right) - \imath\pi \right) \right) \right) \\
= \ & 4\pi\lambda^2 \left( |\mathcal{V}|\kappa^2 + S(\mathcal{V} \cap T(\boldsymbol{s}))\, \kappa \left( \tfrac{1}{8} + \tfrac{\imath}{4\pi} \ln\left( \tfrac{\kappa - k\widehat{\beta}(\boldsymbol{s},k)}{\kappa + k\widehat{\beta}(\boldsymbol{s},k)} \right) \right) \right)
\end{aligned}
\qquad (96)
$$

where again we have used the fact that the circumference of the circle $\mathcal{S}(0, \kappa) \cap \boldsymbol{n}(\boldsymbol{s})^\perp$ is $2\pi\kappa$.

Equation (96) is to be compared to (77), that we obtained in the case of Neumann's boundary condition ($\widehat{\beta} = 0$).

*6.1.3. Integrated pseudo spectrum*

If we assume that the random processes $\zeta(\boldsymbol{y}, \mathcal{V}_1, k)$ and $\zeta(\boldsymbol{y}, \mathcal{V}_2, k)$ are pseudo-uncorrelated as soon as $\mathcal{V}_1 \cap \mathcal{V}_2 = \emptyset$, then by integrating (92) and (96) over all points $\boldsymbol{s} \in \overline{V}$, the isotropic pseudo spectrum of $B$ defined in (70) is

$$\widehat{J}_B(\kappa, k) = \widehat{J}_\zeta(\kappa, \overline{V}, k) = 4\pi\lambda \left( \kappa^2 + \lambda\kappa \left( \frac{S(\partial V)}{8} + \frac{\imath}{4\pi} \int_{\boldsymbol{s}\in\partial V} \ln\left( \frac{\kappa - k\widehat{\beta}(\boldsymbol{s},k)}{\kappa + k\widehat{\beta}(\boldsymbol{s},k)} \right) dS(\boldsymbol{s}) \right) \right) \quad (97)$$

where $dS(\boldsymbol{s})$ denotes the infinitesimal surface element that replaces $S(\mathcal{V} \cap T(\boldsymbol{s}))$ in (96).

Equation (97) is to be compared to (80), that we obtained in the case of Neumann's boundary condition. Note that, similarly to (71), we have

$$\widehat{J}_B(\kappa, k) = \lambda^2 \rho(\kappa, k), \quad (98)$$

where $\rho(\kappa, k)$ denotes the analytic continuation of the asymptotic expansion of the modal density in (39), from a purely imaginary to a complex-valued specific admittance $\widehat{\beta}(\boldsymbol{s}, k)$ [17].

*6.2. Wave numbers distortion*

We will now show that the power spectrum $\widehat{\Gamma}_B(K)$ in (80) and the pseudo spectrum $\widehat{J}_B(\kappa, k)$ in (97) are related through the equation

$$\widehat{\Gamma}_B(K) = \widehat{J}_B(\mathcal{K}(K,k), k)\, \frac{d\mathcal{K}(K,k)}{dK}. \quad (99)$$

In (99), function $K \mapsto \mathcal{K}(K,k)$ is such that $\mathcal{K}(K,0) = K$ and $\mathcal{K}(0,k) = 0$, and it can be interpreted as a distortion of the wave number $K$ when the specific admittance $\widehat{\beta}$ is non-zero.

Indeed, with the change of variable $\kappa = \mathcal{K}(K,k)$ in the right member of (99), integrating (99) w.r.t. $K$ yields

$$\int_0^K \widehat{\Gamma}_B(\kappa) d\kappa = \int_0^{\mathcal{K}(K,k)} \widehat{J}_B(\kappa, k)\, d\kappa. \quad (100)$$

Then substituting (80) and (97) into (100) yields

$$\int_0^K \left( \kappa^2 + \frac{\lambda S(\partial V)}{8}\kappa \right) d\kappa = \int_0^{\mathcal{K}(K,k)} \left( \kappa^2 + \frac{\lambda S(\partial V)}{8}\kappa + \frac{\imath\lambda}{4\pi} \int_{\boldsymbol{s}\in\partial V} \kappa \ln\left( \frac{\kappa - k\widehat{\beta}(\boldsymbol{s},k)}{\kappa + k\widehat{\beta}(\boldsymbol{s},k)} \right) dS(\boldsymbol{s}) \right) d\kappa,$$

which can be rewritten

$$\begin{aligned} &\frac{K^3}{3} + \frac{\lambda S(\partial V)}{8}\frac{K^2}{2} = \frac{\mathcal{K}(K,k)^3}{3} + \frac{\lambda S(\partial V)}{8}\frac{\mathcal{K}(K,k)^2}{2} \\ &+ \frac{\imath\lambda}{4\pi} \int_{\boldsymbol{s}\in\partial V} \left( \frac{\mathcal{K}(K,k)^2}{2} \ln\left( \frac{\mathcal{K}(K,k) - k\widehat{\beta}(\boldsymbol{s},k)}{\mathcal{K}(K,k) + k\widehat{\beta}(\boldsymbol{s},k)} \right) - \frac{k^2\widehat{\beta}(\boldsymbol{s},k)^2}{2} \ln\left( \frac{k\widehat{\beta}(\boldsymbol{s},k) - \mathcal{K}(K,k)}{k\widehat{\beta}(\boldsymbol{s},k) + \mathcal{K}(K,k)} \right) - k\widehat{\beta}(\boldsymbol{s},k)\mathcal{K}(K,k) \right) dS(\boldsymbol{s}). \end{aligned} \quad (101)$$

[17] Equation (98) can be easily proved by using the well-known identity $\arctan(x) = \frac{1}{2\imath} \ln\left( \frac{1+\imath x}{1-\imath x} \right)$.

Equation (101) defines function $\mathcal{K}(K,k)$ implicitly, but it is hardly exploitable. Instead, we will prove that asymptotically (i.e. when $K \to +\infty$), $\mathcal{K}(K,k)$ admits the following asymptotic expansion:

$$\mathcal{K}(K,k) = K + \frac{\imath\lambda}{8\pi}\int_{\boldsymbol{s}\in\partial V}\left(\ln\left(\frac{\mathcal{K}(K,k)+k\widehat{\beta}(\boldsymbol{s},k)}{\mathcal{K}(K,k)-k\widehat{\beta}(\boldsymbol{s},k)}\right) - \left(\frac{k\widehat{\beta}(\boldsymbol{s},k)}{\mathcal{K}(K,k)}\right)^2 \ln\left(\frac{k\widehat{\beta}(\boldsymbol{s},k)+\mathcal{K}(K,k)}{k\widehat{\beta}(\boldsymbol{s},k)-\mathcal{K}(K,k)}\right) + \frac{2k\widehat{\beta}(\boldsymbol{s},k)}{\mathcal{K}(K,k)}\right) dS(\boldsymbol{s}). \tag{102}$$

Indeed, let $\epsilon(K,k) = \mathcal{K}(K,k) - K$, and suppose that $\mathcal{K}(K,k)$ is large with respect to both $\epsilon(K,k)$ and $\lambda S(\partial V)$. Then by substituting $K = \mathcal{K}(K,k) - \epsilon(K,k)$ in the left member of (101) and by then dividing both members by $\mathcal{K}(K,k)^2$, we get

$$\epsilon(K,k) = \frac{\imath\lambda}{8\pi}\int_{\boldsymbol{s}\in\partial V}\left(\ln\left(\frac{\mathcal{K}(K,k)+k\widehat{\beta}(\boldsymbol{s},k)}{\mathcal{K}(K,k)-k\widehat{\beta}(\boldsymbol{s},k)}\right) - \left(\frac{k\widehat{\beta}(\boldsymbol{s},k)}{\mathcal{K}(K,k)}\right)^2 \ln\left(\frac{k\widehat{\beta}(\boldsymbol{s},k)+\mathcal{K}(K,k)}{k\widehat{\beta}(\boldsymbol{s},k)-\mathcal{K}(K,k)}\right) + \frac{2k\widehat{\beta}(\boldsymbol{s},k)}{\mathcal{K}(K,k)}\right) dS(\boldsymbol{s}),$$

which finally proves (102).

We note that function $\mathcal{K}$ in (102) satisfies the following symmetry property:

$$\mathcal{K}(K,-\overline{k}) = \overline{\mathcal{K}(K,k)}. \tag{103}$$

*6.3. Green's function*

The tempered distribution $J_B(\boldsymbol{z},k)$ is such that, for any analytic function $\psi \in \mathcal{S}(\mathbb{R}^3)$,

$$\begin{aligned}\left\langle J_B(\boldsymbol{z},k)\middle|\widehat{\psi}(\boldsymbol{z})\right\rangle &= \left\langle \frac{\widehat{J}_B(\|\boldsymbol{\kappa}\|_2,k)}{4\pi\|\boldsymbol{\kappa}\|_2^2}\middle|\psi(\boldsymbol{\kappa})\right\rangle \\ &= \int_{\boldsymbol{\kappa}\in\mathbb{R}^3} \frac{\widehat{J}_B(\|\boldsymbol{\kappa}\|_2,k)}{4\pi\|\boldsymbol{\kappa}\|_2^2}\,\psi(\boldsymbol{\kappa})\,d\boldsymbol{\kappa} \\ &= \int_{\kappa\in\mathbb{R}_+} \widehat{J}_B(\kappa,k)\,\breve{\psi}(\kappa)\,d\kappa,\end{aligned} \tag{104}$$

where $\frac{\widehat{J}_B(\|\boldsymbol{\kappa}\|_2,k)}{4\pi\|\boldsymbol{\kappa}\|_2^2}$ is the isotropic 3D Fourier transform of $J_B(\boldsymbol{z},k)$ (which sums to $\widehat{J}_B(\|\boldsymbol{\kappa}\|_2,k)$ on the sphere $\mathcal{S}(0,\|\boldsymbol{\kappa}\|_2)$), and $\breve{\psi}(\kappa)$ is a rapidly decreasing analytic function:

$$\breve{\psi}(\kappa) = \frac{1}{4\pi\kappa^2}\int_{\boldsymbol{\kappa}\in\mathcal{S}(0,\kappa)} \psi(\boldsymbol{\kappa})dS(\boldsymbol{\kappa}).$$

Then, by analytic continuation of the pseudo spectrum $\widehat{J}_B(\kappa,k)$ in (97) and of the analytic function $\breve{\psi}(\kappa)$, the Cauchy's integral theorem applied to the last member of (104) proves that

$$\left\langle J_B(\boldsymbol{z},k)\middle|\widehat{\psi}(\boldsymbol{z})\right\rangle = \int_{\kappa\in\mathcal{K}(\mathbb{R}_+,k)} \widehat{J}_B(\kappa,k)\,\breve{\psi}(\kappa)\,d\kappa. \tag{105}$$

Indeed, function $\mathcal{K}(.,k)$ is such that $\lim_{K\to 0_+}\mathcal{K}(K,k) = 0$ and $\lim_{K\to+\infty}\mathcal{K}(K,k) - K = 0$, and $\forall K > 0$, function $\kappa \mapsto \widehat{J}_B(\kappa,k)$ in (97) is holomorphic inside the simply closed contour $\mathcal{C} = [0,K] \cup \mathcal{K}([0,K],k) \cup [K,\mathcal{K}(K,k)]$.

By applying the change of variable $\kappa = \mathcal{K}(K,k)$ in (105), we then get

$$\begin{aligned}\left\langle J_B(\boldsymbol{z},k)\middle|\widehat{\psi}(\boldsymbol{z})\right\rangle &= \int_{K\in\mathbb{R}_+} \widehat{J}_B(\mathcal{K}(K,k),k)\,\breve{\psi}(\mathcal{K}(K,k))\,\frac{d\mathcal{K}(K,k)}{dK}dK \\ &= \int_{K\in\mathbb{R}_+} \widehat{\Gamma}_B(K)\,\breve{\psi}(\mathcal{K}(K,k))\,dK\end{aligned} \tag{106}$$

where we have substituted (99).

In other respects, equation (13) shows that

$$J_B(\boldsymbol{z},k) = \left(\Delta + 4\pi^2 k^2\right)^2 J_G(\boldsymbol{z},k). \tag{107}$$

We deduce from (106) and (107) that

$$\left\langle J_G(\boldsymbol{z},k) \middle| \left(\Delta + 4\pi^2 k^2\right)^2 \widehat{\psi}(\boldsymbol{z}) \right\rangle = \left\langle J_B(\boldsymbol{z},k) \middle| \widehat{\psi}(\boldsymbol{z}) \right\rangle = \int_{K\in\mathbb{R}_+} \widehat{\Gamma}_B(K)\, \breve{\psi}(\mathcal{K}(K,k))\, dK. \tag{108}$$

Therefore the tempered distribution $J_G(\boldsymbol{z},k)$ can equivalently be written as a function:

$$J_G(\boldsymbol{z},k) = \int_{K\in\mathbb{R}_+} \frac{\operatorname{sinc}(2\pi\mathcal{K}(K,k)\|\boldsymbol{z}\|_2)}{\left(4\pi^2(\mathcal{K}(K,k)^2 - k^2)\right)^2} \widehat{\Gamma}_B(K)\, dK, \tag{109}$$

which indeed satisfies equation (108) [18].

Then, if we assume that the spectral representation of the random process $G(\boldsymbol{x},k)$ is a distortion of the spectral representation (81) that we obtained in the case of Neumann's boundary condition, we can write

$$G(\boldsymbol{x},k) = \mu_G(k) + \int_{\boldsymbol{k}\in\mathbb{R}^3} \int_{\boldsymbol{s}\in\overline{V}} \frac{e^{2\imath\pi \frac{\mathcal{K}(\|\boldsymbol{k}\|_2,k)}{\|\boldsymbol{k}\|_2} \boldsymbol{k}^\top(\boldsymbol{x}-\boldsymbol{s})}}{4\pi^2(\mathcal{K}(\|\boldsymbol{k}\|_2,k)^2 - k^2)} d\widehat{\xi}^0(\boldsymbol{k},\boldsymbol{s}), \tag{110}$$

where $\widehat{\xi}^0$ denotes the same complex random measure as in (81), and with the same mean as in (82): $\mu_G(k) = \mu_B(k)\, \widehat{G}_0(\boldsymbol{0},k) = -\frac{\lambda}{4\pi^2 k^2}$, where $\mu_B(k) = \lambda$ was given in (69).

Indeed, the PCF of $G(\boldsymbol{x},k)$ in (110) satisfies (109):

$$\begin{aligned}
\operatorname{cov}[G(\boldsymbol{x}_1,k), \overline{G(\boldsymbol{x}_2,k)}] &= \int_{\boldsymbol{k}\in\mathbb{R}^3} \int_{\boldsymbol{s}\in\overline{V}} \frac{e^{2\imath\pi \frac{\mathcal{K}(\|\boldsymbol{k}\|_2,k)}{\|\boldsymbol{k}\|_2} \boldsymbol{k}^\top(\boldsymbol{x}_1-\boldsymbol{s})}}{4\pi^2(\mathcal{K}(\|\boldsymbol{k}\|_2,k)^2-k^2)} \frac{e^{-2\imath\pi \frac{\mathcal{K}(\|\boldsymbol{k}\|_2,k)}{\|\boldsymbol{k}\|_2} \boldsymbol{k}^\top(\boldsymbol{x}_2-\boldsymbol{s})}}{4\pi^2(\mathcal{K}(\|\boldsymbol{k}\|_2,k)^2-k^2)} \frac{d\widehat{\Lambda}^0(\|\boldsymbol{k}\|_2,\boldsymbol{s})}{4\pi\|\boldsymbol{k}\|_2^2} d\boldsymbol{k} \\
&= \int_{\boldsymbol{k}\in\mathbb{R}^3} \frac{e^{2\imath\pi \frac{\mathcal{K}(\|\boldsymbol{k}\|_2,k)}{\|\boldsymbol{k}\|_2} \boldsymbol{k}^\top(\boldsymbol{x}_1-\boldsymbol{x}_2)}}{(4\pi^2(\mathcal{K}(\|\boldsymbol{k}\|_2,k)^2-k^2))^2} \frac{\widehat{\Lambda}^0(\|\boldsymbol{k}\|_2,\overline{V})}{4\pi\|\boldsymbol{k}\|_2^2} d\boldsymbol{k} \\
&= J_G(\boldsymbol{x}_1-\boldsymbol{x}_2,k),
\end{aligned}$$

due to (65).

Finally, note that the expression of $G(\boldsymbol{x},k)$ in equation (110) involves function $\mathcal{K}(K,k)$ defined in (102), which depends analytically on $\widehat{\beta}$. Even though (110) has been established by assuming that $\operatorname{Im}(\widehat{\beta}) < 0$ (which permitted us to use the expression of the $B$-function in (29)), in other respects we know that the Green's function of the Helmholtz equation, in the case of the Robin boundary condition with a Lipschitz continuous boundary, is an analytic function of the specific admittance[19] $\widehat{\beta}$. Therefore we can conclude that the same formula (110) also holds when $\operatorname{Im}(\widehat{\beta}) > 0$.

---

[18](108) can be retrieved from (109) by using the identity $\left(\Delta + 4\pi^2 k^2\right)^2 \left(\frac{\operatorname{sinc}(2\pi\mathcal{K}(K,k)\|\boldsymbol{z}\|_2)}{(4\pi^2(\mathcal{K}(K,k)^2-k^2))^2}\right) = \operatorname{sinc}(2\pi\mathcal{K}(K,k)\|\boldsymbol{z}\|_2)$.

[19]The analyticity of function $G(\boldsymbol{x},\boldsymbol{x}_0,k)$ in (33) w.r.t. $\widehat{\beta}$ is a corollary of Theorem 1.1 in (Bögli *et al.*, 2022).

*6.4. Source response*

Substituting (110) into (8) leads to

$$\dot{g}(\boldsymbol{x},t) = \mu_{\dot{g}}(t) - c^2 \int_{\boldsymbol{k}\in\mathbb{R}^3} \int_{\boldsymbol{s}\in\overline{V}} \left( \int_{f\in\mathbb{R}} \frac{2\imath\pi f\, e^{2\imath\pi \frac{\mathcal{K}(\|\boldsymbol{k}\|_2, \frac{f}{c})}{\|\boldsymbol{k}\|_2} \boldsymbol{k}^\top(\boldsymbol{x}-\boldsymbol{s})}}{4\pi^2(f^2 - c^2\mathcal{K}(\|\boldsymbol{k}\|_2, \frac{f}{c})^2)} e^{2\imath\pi f t} df \right) d\widehat{\xi}^0(\boldsymbol{k},\boldsymbol{s}) \quad (111)$$

with $\mu_{\dot{g}}(t)$ as in (84).

Let $\kappa(k) \in \mathbb{C}$ be the unique solution to the equation $\kappa(k) = \mathcal{K}(k, \kappa(k))$ with both nonnegative real and imaginary parts. Then because of the symmetry property (103), we get $\mathcal{K}(k, -\overline{\kappa(k)}) = \overline{\kappa(k)}$. Then the equation $f^2 = c^2\mathcal{K}(k, \frac{f}{c})^2$ admits two solutions $f = c\kappa(k)$ and $f = -c\overline{\kappa(k)}$, which are both in the upper half complex plane.

By applying the residue theorem to (111), we thus get[20]:

$$\dot{g}(\boldsymbol{x},t) = \mu_{\dot{g}}(t) + c^2 H(t)\,\mathrm{Re}\left( \int_{\boldsymbol{k}\in\mathbb{R}^3} \int_{\boldsymbol{s}\in\overline{V}} e^{2\imath\pi\left(\frac{\kappa(\|\boldsymbol{k}\|_2)}{\|\boldsymbol{k}\|_2}\boldsymbol{k}^\top(\boldsymbol{x}-\boldsymbol{s}) + c\,\kappa(\|\boldsymbol{k}\|_2)t\right)} d\widehat{\xi}^0(\boldsymbol{k},\boldsymbol{s}) \right) \quad (112)$$

where we have used the symmetry property (103). By substituting (84) and (112) into (36), we retrieve (86), with the following spectral representation of $q$:

$$q(\boldsymbol{x},t) = c^2 \left( \lambda + \mathrm{Re}\left( \int_{\boldsymbol{k}\in\mathbb{R}^3} \int_{\boldsymbol{s}\in\overline{V}} e^{2\imath\pi\left(\frac{\kappa(\|\boldsymbol{k}\|_2)}{\|\boldsymbol{k}\|_2}\boldsymbol{k}^\top(\boldsymbol{x}-\boldsymbol{s}) + c\,\kappa(\|\boldsymbol{k}\|_2)t\right)} d\widehat{\xi}^0(\boldsymbol{k},\boldsymbol{s}) \right) \right) \quad (113)$$

which is to be compared to the discrete expression (37) established before spectral smoothing, and which generalizes (87) that we obtained in the case of Neumann's boundary condition to $\widehat{\beta} \neq 0$. Based on (113), the ACF of $q$ defined in (45) is a tempered distribution, so that $\forall \psi(f) \in \mathcal{S}(\mathbb{R})$ such that $\psi(0) = 0$ at $f = 0$ (remember that we are working under the high frequency Assumption 2),

$$\left\langle \Gamma_q(\boldsymbol{x}_1, \boldsymbol{x}_2, t+\tfrac{\tau}{2}, t-\tfrac{\tau}{2}) \middle| \widehat{\psi}(\tau) \right\rangle = \tfrac{c^4}{4} \int_{k\in\mathbb{R}_+} \int_{\boldsymbol{s}\in\overline{V}} e^{-4\pi c\,\mathrm{Im}(\kappa(k))t} \Big( \gamma(\boldsymbol{x}_1-\boldsymbol{s}, \boldsymbol{x}_2-\boldsymbol{s}, \kappa(k))\, \psi(c\mathrm{Re}(\kappa(k))) + \overline{\gamma(\boldsymbol{x}_1-\boldsymbol{s}, \boldsymbol{x}_2-\boldsymbol{s}, \kappa(k))}\, \psi(-c\mathrm{Re}(\kappa(k))) \Big)\, d\widehat{\Lambda}^0(k,\boldsymbol{s})dk \quad (114)$$

where the spectral measure $\widehat{\Lambda}^0(\boldsymbol{k}, \mathcal{V})$ was defined in (79), and function $\gamma$ is defined as $\forall \boldsymbol{y}_1, \boldsymbol{y}_2 \in \mathbb{R}^3$, $\forall \kappa \in \mathbb{C}$,

$$\gamma(\boldsymbol{y}_1, \boldsymbol{y}_2, \kappa) = \mathrm{sinc}\left( 2\pi \sqrt{(\kappa\boldsymbol{y}_1 - \overline{\kappa}\boldsymbol{y}_2)^\top (\kappa\boldsymbol{y}_1 - \overline{\kappa}\boldsymbol{y}_2)} \right) \quad (115)$$

[20] Actually, the expression in (112) is incomplete, because function $f \mapsto e^{2\imath\pi \frac{\mathcal{K}(\|\boldsymbol{k}\|_2, \frac{f}{c})}{\|\boldsymbol{k}\|_2} \boldsymbol{k}^\top(\boldsymbol{x}-\boldsymbol{s})}$ in the numerator of the fraction in (111) has its own singularities. As we did in Section (3.4.2) regarding function $f \mapsto \varphi_n(\boldsymbol{x}_0, \frac{f}{c})\,\varphi_n(\boldsymbol{x}, \frac{f}{c})$ in (34) (*cf.* footnote 7), we will ignore these singularities, which amounts to assume that none of them is located below the set of poles $\cup_{k\in\mathbb{R}_+}\{c\kappa(k)\}$ when $\mathrm{Re}(\kappa) \to +\infty$.

where sinc(.) denotes the analytic continuation of the cardinal sine function on $\mathbb{C}$, and $\sqrt{(.)}$ can denote any of the two complex square roots of opposite sign, since function sinc(.) in (115) is even. Function $\gamma$ defined in (115) generalizes the $\gamma$ function (44) of the spectral correlation introduced in Section 3.6.4. Finally, equation (114) generalizes equation (88) that we obtained in the case of Neumann's boundary condition to $\widehat{\beta} \neq 0$.

### *6.5. Simplification of the wave numbers distortion*

In Section 6.4, $\kappa(k)$ was defined as the unique solution to the equation $\kappa(k) = \mathcal{K}(k, \kappa(k))$ with both nonnegative real and imaginary parts. Then by substituting $K \leftarrow k$ and $k \leftarrow \kappa(k)$ into equation (102), we get the asymptotic expansion

$$\kappa(k) = k + \tfrac{\imath\lambda}{8\pi} \int_{\boldsymbol{s}\in\partial V} \left(\ln\left(\tfrac{1+\widehat{\beta}(\boldsymbol{s},\kappa(k))}{1-\widehat{\beta}(\boldsymbol{s},\kappa(k))}\right) - \widehat{\beta}(\boldsymbol{s},\kappa(k))^2 \ln\left(\tfrac{\widehat{\beta}(\boldsymbol{s},\kappa(k))+1}{\widehat{\beta}(\boldsymbol{s},\kappa(k))-1}\right) + 2\widehat{\beta}(\boldsymbol{s},\kappa(k))\right) dS(\boldsymbol{s}). \tag{116}$$

Equation (116) provides an implicit expression of function $\kappa(k)$. In addition, if we further assume that function $\widehat{\beta}$ never gets close to 1, that it is bounded, and that $\lim_{k\to+\infty} \frac{d\widehat{\beta}(\boldsymbol{s},k)}{dk} = 0$, then (116) can be simplified into an explicit expression:

$$\kappa(k) = k + \tfrac{\imath\lambda}{8\pi} \int_{\boldsymbol{s}\in\partial V} \left(\ln\left(\tfrac{1+\widehat{\beta}(\boldsymbol{s},k)}{1-\widehat{\beta}(\boldsymbol{s},k)}\right) - \widehat{\beta}(\boldsymbol{s},k)^2 \ln\left(\tfrac{\widehat{\beta}(\boldsymbol{s},k)+1}{\widehat{\beta}(\boldsymbol{s},k)-1}\right) + 2\widehat{\beta}(\boldsymbol{s},k)\right) dS(\boldsymbol{s}). \tag{117}$$

Note that the wave number distortion in (117) can equivalently be written in the following form:

$$\kappa(k) = k + \tfrac{\imath\lambda}{4\pi} \int_{\boldsymbol{s}\in\partial V} \left(\int_{u=0}^{1} \ln\left(\tfrac{u+\widehat{\beta}(\boldsymbol{s},k)}{u-\widehat{\beta}(\boldsymbol{s},k)}\right) u\, du\right) dS(\boldsymbol{s}),$$

which implies

$$\mathrm{Im}(\kappa(k)) = \tfrac{\lambda}{8\pi} \int_{\boldsymbol{s}\in\partial V} \left(\int_{u=0}^{1} \ln\left(\left|\tfrac{u+\widehat{\beta}(\boldsymbol{s},k)}{u-\widehat{\beta}(\boldsymbol{s},k)}\right|^2\right) u\, du\right) dS(\boldsymbol{s}). \tag{118}$$

Since $\mathrm{Re}(\widehat{\beta}(\boldsymbol{s},k)) \geq 0$, this last expression confirms that $\mathrm{Im}(\kappa(k))$ is nonnegative.

### *6.6. Wigner distribution*

By substituting (114) into (46), we get the asymptotic expansion of the Wigner distribution of the random process $q$, which holds when $f \to +\infty$:

$$W_q(\boldsymbol{x}_1, \boldsymbol{x}_2, f, t) = \tfrac{c^4}{4} \int_{l\in\mathbb{R}_+} \delta(f - c\mathrm{Re}(\kappa(l)) e^{-4\pi c \mathrm{Im}(\kappa(l))t} \int_{\boldsymbol{s}\in\overline{V}} \gamma(\boldsymbol{x}_1 - \boldsymbol{s}, \boldsymbol{x}_2 - \boldsymbol{s}, \kappa(l))\, d\widehat{\Lambda}^0(l, \boldsymbol{s}) dl \tag{119}$$

where $\gamma(.)$ was defined in (115) and the spectral measure $\widehat{\Lambda}^0(l, \mathcal{V})$ in (79). With the change of variable $k = \mathrm{Re}(\kappa(l))$, equation (119) yields asymptotically:

$$W_q(\boldsymbol{x}_1, \boldsymbol{x}_2, f, t) = \tfrac{c^3}{4} e^{-4\pi c \mathrm{Im}(\kappa(\frac{f}{c}))t} \int_{\boldsymbol{s}\in\overline{V}} \gamma\left(\boldsymbol{x}_1 - \boldsymbol{s}, \boldsymbol{x}_2 - \boldsymbol{s}, \tfrac{f}{c} + \imath \mathrm{Im}(\kappa(\tfrac{f}{c}))\right) d\widehat{\Lambda}^1(\tfrac{f}{c}, \boldsymbol{s}), \tag{120}$$

where the distorted spectral measure $\widehat{\Lambda}^1(k,\mathcal{V})$ is expressed as

$$\widehat{\Lambda}^1(k,\mathcal{V}) = \frac{\widehat{\Lambda}^0((\mathrm{Re}\kappa)^{-1}(k),\mathcal{V})}{(\mathrm{Re}\kappa)'((\mathrm{Re}\kappa)^{-1}(k))}. \tag{121}$$

In addition, equation (120) can be rewritten

$$W_q(\boldsymbol{x}_1,\boldsymbol{x}_2,f,t) = W_q(\boldsymbol{x}_1,\boldsymbol{x}_2,f)\, e^{-2\alpha(\frac{f}{c})t} \tag{122}$$

where

$$W_q(\boldsymbol{x}_1,\boldsymbol{x}_2,f) \triangleq W_q(\boldsymbol{x}_1,\boldsymbol{x}_2,f,0) = \tfrac{c^3}{4}\int_{\boldsymbol{s}\in\overline{V}} \gamma\left(\boldsymbol{x}_1-\boldsymbol{s},\boldsymbol{x}_2-\boldsymbol{s},\tfrac{f}{c}+\imath\mathrm{Im}(\kappa(\tfrac{f}{c}))\right) d\widehat{\Lambda}^1(\tfrac{f}{c},\boldsymbol{s}) \tag{123}$$

and (117) yields the expression of the spectral attenuation:

$$\begin{aligned}\alpha(k) \triangleq{}& 2\pi c\,\mathrm{Im}(\kappa(k))\\ ={}& \tfrac{\lambda c}{8}\int_{\boldsymbol{s}\in\partial V}\left(\ln\left(\left|\tfrac{1+\widehat{\beta}(\boldsymbol{s},k)}{1-\widehat{\beta}(\boldsymbol{s},k)}\right|^2\right)+2\mathrm{Re}\left(\widehat{\beta}(\boldsymbol{s},k)\left(2-\widehat{\beta}(\boldsymbol{s},k)\ln\left(\tfrac{\widehat{\beta}(\boldsymbol{s},k)+1}{\widehat{\beta}(\boldsymbol{s},k)-1}\right)\right)\right)\right)dS(\boldsymbol{s}).\end{aligned}$$

We note that the Wigner distribution $W_q(\boldsymbol{x}_1,\boldsymbol{x}_2,f,t)$ in (122) has the same factorized form as the Polack time-frequency distribution (43) (which was originally known only for $\boldsymbol{x}_1=\boldsymbol{x}_2$), introduced in Section 3.6.3. Moreover, we get the closed-form expression of the reverberation time in mixing rooms:

$$T_{60}(f) \triangleq \tfrac{3\ln(10)}{\alpha(\frac{f}{c})} = \tfrac{24\ln(10)}{c}\frac{|V|}{\int_{\boldsymbol{s}\in\partial V}\left(\ln\left(\left|\frac{1+\widehat{\beta}(\boldsymbol{s},\frac{f}{c})}{1-\widehat{\beta}(\boldsymbol{s},\frac{f}{c})}\right|^2\right)+2\mathrm{Re}\left(\widehat{\beta}(\boldsymbol{s},\frac{f}{c})\left(2-\widehat{\beta}(\boldsymbol{s},\frac{f}{c})\ln\left(\frac{\widehat{\beta}(\boldsymbol{s},\frac{f}{c})+1}{\widehat{\beta}(\boldsymbol{s},\frac{f}{c})-1}\right)\right)\right)\right)dS(\boldsymbol{s})}. \tag{124}$$

Equation (124) may look hardly interpretable, but actually equation (118) shows that (124) can be rewritten in exactly the same form as Eyring's formula (41), provided that the average absorption coefficient $a(\boldsymbol{s},f)$ is defined so that

$$1-a(\boldsymbol{s},f) = \exp\left(\langle\ln\left(1-a(\boldsymbol{s},f,u)\right)\rangle\right), \tag{125}$$

with

$$\langle\ln\left(1-a(\boldsymbol{s},f,u)\right)\rangle = \frac{\int_{u=0}^1 \ln(1-a(\boldsymbol{s},f,u))u\,du}{\int_{u=0}^1 u\,du} = \int_{\theta=0}^{\frac{\pi}{2}} \ln\left(1-a(\boldsymbol{s},f,\cos(\theta))\right)\sin(2\theta)\,d\theta. \tag{126}$$

In (126), $\langle\ln(1-a(\boldsymbol{s},f,u))\rangle$ denotes the average value of $\ln(1-a(\boldsymbol{s},f,u))$ for all possible angles of incidence $\theta$, where the angle-dependent absorption coefficient $a(\boldsymbol{s},f,u)$ with $u=\cos(\theta)$ was defined in (28). This average is weighted by $u$, which is proportional to the *apparent area* of the surface element $dS(\boldsymbol{s})$ for the incident plane wave of angle $\theta$.

Note that the expression of the average absorption coefficient $a(\boldsymbol{s},f)$ in (125) involves a geometric mean rather than an arithmetic mean over all angles of incidence. However, when the absorption coefficient $a(\boldsymbol{s}, f, u)$ is small, equations (124), (125) and (126) lead exactly to Sabine's formula (40), where $a(\boldsymbol{s}, f) = \int_{\theta=0}^{\frac{\pi}{2}} a(\boldsymbol{s}, f, \cos(\theta)) \sin(2\theta)\, d\theta$ is exactly the Paris formula of the average absorption coefficient for a random and uniformly distributed sound incidence (Kuttruff, 2014, Chapter 2).

Finally, when $\boldsymbol{x}_1 = \boldsymbol{x}_2$, by substituting (115) into (123), we get the simplified expression of the power distribution over space at frequency $f$:

$$W_q(\boldsymbol{x}, \boldsymbol{x}, f) = \tfrac{c^3}{4} \int_{\boldsymbol{s} \in \overline{V}} \operatorname{sinhc}\left(4\pi \operatorname{Im}(\kappa(\tfrac{f}{c})) \|\boldsymbol{x} - \boldsymbol{s}\|_2\right) d\widehat{\Lambda}^1(\tfrac{f}{c}, \boldsymbol{s})$$

where sinhc denotes the hyperbolic cardinal sine function: $\operatorname{sinhc}(u) = \frac{\sinh(u)}{u}$.

Since the sinhc function is strictly convex, $W_q(\boldsymbol{x}, \boldsymbol{x}, f)$ is a strictly convex function of $\boldsymbol{x}$ (as a sum of strictly convex functions), which reaches its minimum value at some point $\boldsymbol{x}_{\min}$ which is a weighted mean of all points in $\overline{V}$. Moreover, function $W_q(\boldsymbol{x}, \boldsymbol{x}, f)$ increases exponentially with the distance $\|\boldsymbol{x} - \boldsymbol{x}_{\min}\|$. However, we should keep in mind that the location information has been smoothed when we averaged the statistics of the $B$-function over space, so $W_q(\boldsymbol{x}, \boldsymbol{x}, f)$ is a smoothed power distribution over space. In future work, the expression of this power distribution will be refined, by introducing the curvature and the edge terms in the asymptotic expansion (see Section 7).

## 7. Limitations of the approach and future work

In this section, we discuss some current limitations of the Statistical Wave Field Theory, and show how they will be overcome in future work.

### *7.1. Non-mixing billiards*

In this paper, we have addressed the most usual case of mixing billiards, where the position $\boldsymbol{x}(t)$ and the direction $\boldsymbol{d}(t)$ of any ray trajectory are jointly uniformly distributed in the phase space $V \times \mathcal{S}(0, 1)$ (*cf.* Section 3.6.1). This property is related to the geometric shape of the domain, and it has been translated into the language of the probability theory through Assumptions 1 and 3 in Section 4. As explained in Section 3.5.2, it guarantees that the oscillations in the power spectrum $\widehat{\Gamma}_B$ (or in the pseudo spectrum $\widehat{J}_B$), which are not accounted for in equations (80) and (97), are indeed negligible. However, some common geometric shapes are non-mixing, so it will be interesting to study how the Statistical Wave Field Theory can be generalized to such geometries.

For instance, we will address the case of non-mixing and non-ergodic billiards, in which the position space $V$ is still explored in a mixing manner by any ray trajectory, but not the direction space $\mathcal{S}(0, 1)$. This is e.g. the case of the cuboid, where almost all trajectories reach almost all positions, but only take eight different directions (Polack, 1992). Assumption 3 will then be relaxed: the isotropy assumption will be replaced by a detailed mathematical study of the dynamical process which leads to a complete isotropy in the case of mixing billiards, and which is left incomplete in other geometric shapes. We will then show that the wave vector space is distorted in an anisotropic way when the specific admittance is non-zero, resulting in an exponential decay rate that depends not only on the wave number, but also on the wave vector direction.

In other respects, Polack (1992) also mentions the case of billiards whose phase space breaks down into a finite number of distinct subsets. In this case, each trajectory explores one subset only, in a mixing manner. The Statistical Wave Field Theory can be adapted to this kind of billiard, by computing different space-averaged statistics of the $B$-function in every subset.

### *7.2. Wave-related phenomena*

In this paper, the Statistical Wave Field Theory has been introduced as a high frequency approximation (*cf.* Section 4.3), which holds under the same conditions as geometric acoustics and optics. This permitted us to approximate wave propagation by considering the trajectory of rays that undergo successive specular reflections, and to establish a relationship with the mathematical theory of dynamical billiards (*cf.* Section 3.6.1).

However, it is well known that the sound ray interpretation does not hold at lower frequencies, because it ignores wave-related phenomena, such as edge diffraction. In order to take wave phenomena into account, we will need to pursue the asymptotic expansions introduced in Sections 5.1 and 6.1 up to the second order.

When the boundary $\partial V$ is twice continuously differentiable, considering the relationships between the power spectrum $\widehat{\Gamma}_B(k)$ and the modal density $\rho(k, 0)$ in (71) on the one hand, and the pseudo spectrum $\widehat{J}_B(\kappa, k)$ and the modal density $\rho(\kappa, k)$ in (98) on the other hand, we will introduce a second order *curvature term* as in (Balian and Bloch, 1970), which indeed involves non-specular reflections.

Moreover, in order to explicitly account for edge diffraction, when the boundary is piecewise twice continuously differentiable with edges and vertices, which is e.g. the case of polyhedral surfaces, we will show that vertices actually generate negligible terms in the asymptotic expansion, whereas edges generate a second order *edge term*, which will be expressed in closed-form.

Equipped with the two *curvature* and *edge* second order terms, the predictions of the Statistical Wave Field Theory will then hold more accurately at lower frequencies.

### *7.3. Other limitations*

Some other limitations of the basic version of the Statistical Wave Field Theory presented in this paper are related to the other physical assumptions that we mentioned in the introduction (Section 1) and at the beginning of Section 3.4:

- We assumed that the medium was free of losses. So in room acoustics, the attenuation of sound in air is ignored in the expression of the reverberation time (124), whereas it is often taken into account via a very simple correction term brought to Sabine and Eyring's equations (40) and (41) (Kuttruff, 2014, Chapter 5). A similar correction term could be introduced in the Statistical Wave Field Theory.

- We assumed that the wave equation holds exactly in the whole domain $V$, which means that the medium is homogeneous and at rest, in addition to being lossless. So wave phenomena related to changes or fluctuations in the medium, such as refraction and dispersion, were not considered. However, modeling a weakly turbulent or inhomogeneous medium is of the utmost importance in certain applications including underwater acoustics, and could be achieved in future work, *e.g.* by introducing random scatterers as in several studies (Middleton, 1967a,b; Ol'shevskii, 1978; Middleton, 1987; Ratilal and Makris, 2005; Abraham, 2019).

- We have considered omnidirectional punctual sources, and in future work the spatial spread and the directivity of realistic physical sources could be accounted for. Moreover, in practical applications, signal measurements involve sensors, or sensor arrays, and the response and directivity of these sensors could also be accounted for, as in (Middleton, 1967a,b) for instance.

- In this paper, all parameters of the problem, including the random source position and the boundaries of the domain, were assumed constant over time, which excludes any kind of Doppler effect. In future work, we could consider modeling moving sources, receivers, medium, and boundaries (Middleton, 1967a,b; Ol'shevskii, 1978; Middleton, 1987; Abraham, 2019; Goodman, 2000; Jakeman and Ridley, 2006).

- In room acoustics, as mentioned in Section 3.4, Robin's boundary condition as formulated in (25) and (26) amounts to assuming that the room surfaces are locally reacting, which means that the specific admittance $\widehat{\beta}(\boldsymbol{x}, k)$ does not depend on the angle of sound incidence. However, there is no mathematical difficulty in relaxing this assumption by making $\widehat{\beta}$ depend on the wave vector $\boldsymbol{k}$ instead of the wave number $k$.

Last, we have only investigated the first and second order statistics of the source response. However, it is well known in acoustics that the statistics of reverberation are asymptotically normal (Middleton, 1967b; Badeau, 2019). To retrieve this property, higher order statistics could also be investigated, by remarking that the random process $\boldsymbol{y} \mapsto \xi(\boldsymbol{y}, \boldsymbol{s})$, involved in the spectral representation of the source response and introduced in Section 4.4.1, is actually a simple point process, at both interior and boundary points $\boldsymbol{s}$ (see Sections 5.1.1 and 5.1.2).

## 8. Conclusion

In this paper, we have presented the foundations of the Statistical Wave Field Theory, which for the first time establishes mathematically the statistical properties of the solutions to the wave equation in a bounded volume, after many reflections on the boundary surface, in terms of power distribution and correlations, jointly over time, frequency, and space. The first and second order statistics of the wave field have been expressed in closed-form, via asymptotic expansions that hold at high frequency, w.r.t. the geometry and the specific admittance of the boundary surface. In particular, the properties of second order statistics have been highlighted by calculating the Wigner time-frequency distribution between two space positions.

In room acoustics, the Statistical Wave Field Theory has permitted us to retrieve the well-known statistical properties of reverberation that hold in the mixing case, which provides a first confirmation of the theory predictions, through the experimental work of scientists from the 19th and 20th centuries. However, the theory predictions go far beyond these few properties, and even though they have been derived mathematically from the wave equation and its boundary conditions, they still need to be tested by experiments in future work[21].

In Section 7, we have listed several limitations of the current version of the theory, and proposed future developments that should permit us to overcome these limitations. Other possible extensions of the Statistical Wave Field theory include the ones that were mentioned by Balian and Bloch (1970) regarding the asymptotic expansion of the modal density: the generalization of the theory to a space of arbitrary dimension, and its extension from scalar to vector waves in order to represent electromagnetic fields, as in (Balian and Bloch, 1971), as well as the transposition of the theory to other equations of physics, such as the Schrödinger equation, which can also be formulated as a Sturm-Liouville problem.

## Acknowledgments

The author would like to warmly thank the anonymous reviewers for their suggestions and for pointing out very interesting questions regarding the physical assumptions, interpretation and implications of the Statistical Wave Field Theory. The author also thanks one of the reviewers for bringing to his attention the rich bibliography on related works in underwater acoustics, optics and some other fields.

## Author Declarations

*Conflict of Interest:* The author of this paper has no conflict of interest to disclose.

## Data Availability

Data sharing is not applicable to this article as no new data were created or analyzed in this study.

## References

Abraham, D. A. (**2019**). *Underwater acoustic signal processing: Modeling, detection, and estimation* (ASA Press and Springer, New York, NY, USA), 834 pages.

Ahlfors, L. (**1979**). *Complex Analysis* (McGraw-Hill, New York, NY, USA).

[21] A few unpublished experiments have already been carried out by the author of this paper, that confirm the factorized form of the Wigner distribution (122) for two different space positions $\boldsymbol{x}_1$ and $\boldsymbol{x}_2$ in a mixing room.

Allen, J. B., and Berkley, D. A. (**1979**). "Image method for efficiently simulating small-room acoustics," The Journal of the Acoustical Society of America **65**(4), 943–950.

Arendt, W., Nittka, R., Peter, W., and Steiner, F. (**2009**). *Mathematical Analysis of Evolution, Information, and Complexity*, Chap. 1 Weyl's Law: Spectral Properties of the Laplacian in Mathematics and Physics, 1–71 (Wiley-VCH, Weinheim, Germany).

Badeau, R. (**2019**). "Common mathematical framework for stochastic reverberation models," The Journal of the Acoustical Society of America **145**(4), 2733–2745.

Balian, R., and Bloch, C. (**1970**). "Distribution of eigenfrequencies for the wave equation in a finite domain: I. Three-dimensional problem with smooth boundary surface," Annals of Physics **60**(2), 401–447.

Balian, R., and Bloch, C. (**1971**). "Distribution of eigenfrequencies for the wave equation in a finite domain: II. Electromagnetic field. Riemannian spaces," Annals of Physics **64**(1), 271–307.

Balian, R., and Bloch, C. (**1972**). "Distribution of eigenfrequencies for the wave equation in a finite domain: III. Eigenfrequency density oscillations," Annals of Physics **69**(1), 76–160.

Besnier, P., and Démoulin, B. (**2011**). *Electromagnetic Reverberation Chambers* (ISTE/Wiley, New York).

Bögli, S., Kennedy, J. B., and Lang, R. (**2022**). "On the eigenvalues of the Robin Laplacian with a complex parameter," Analysis and Mathematical Physics **12**(1).

Bunimovich, L. (**1979**). "On the ergodic properties of nowhere dispersing billiard," Communications in Mathematical Physics **65**(3), 295–312.

Cohen, L. (**1989**). "Time-frequency distributions-a review," Proc. IEEE **77**(7), 941–981.

Colosi, J. A. (**2016**). *Sound Propagation through the Stochastic Ocean* (Cambridge University Press), 444 pages.

Cook, R. K., Waterhouse, R., Berendt, R., Edelman, S., and Thompson, M. (**1955**). "Measurement of correlation coefficients in reverberant sound fields," The Journal of the Acoustical Society of America **27**(6), 1072–1077.

Daley, D. J., and Vere-Jones, D. (**2003**). Probability and its Applications *An introduction to the theory of point processes. Volume I: Elementary Theory and Methods*, Second ed. (Springer-Verlag, New York).

Eyring, C. F. (**1930**). "Reverberation time in "dead" rooms," The Journal of the Acoustical Society of America **1**(2A), 217–241.

Goodman, J. (**2000**). *Statistical optics* (John Wiley and Sons, New York), 550 pages.

Ishimaru, A. (**1978**a). *Wave propagation and scattering in random media. Vol I: Single scattering and transport theory.* (Academic Press, New York), 250 pages.

Ishimaru, A. (**1978**b). *Wave propagation and scattering in random media. Vol II: Multiple scattering, turbulence, rough surfaces, and remote sensing.* (Academic Press, New York), 572 pages.

Jakeman, E., and Ridley, K. D. (**2006**). *Modeling fluctuations in scattered waves* (Taylor and Francis, London), 313 pages.

Joyce, W. B. (**1975**). "Sabine's reverberation time and ergodic auditoriums," The Journal of the Acoustical Society of America **58**(3), 643–655.

Kuttruff, H. (**2014**). *Room Acoustics, Fifth Edition* (CRC Press, Boca Raton, FL, USA), pp. 1–374.

Middleton, D. (**1967**a). "A statistical theory of reverberation and similar first-order scattered fields–I: Waveforms and the general process," IEEE Transactions on Information Theory **13**(3), 372–392.

Middleton, D. (**1967**b). "A statistical theory of reverberation and similar first-order scattered fields–II: Moments, spectra and special distributions," IEEE Transactions on Information Theory **13**(3), 393–414.

Middleton, D. (**1987**). "Channel modeling and threshold signal processing in underwater acoustics: An analytical overview," IEEE Journal of Oceanic Engineering **12**(1), 4–28.

Moorer, J. A. (**1979**). "About this reverberation business," Computer Music Journal **3**(2), 13–28.

Morse, P. M., and Ingard, K. U. (**1968**). *Theoretical acoustics* (McGraw-Hill, New York, NY, USA).

Ochmann, M. (**2004**). "The complex equivalent source method for sound propagation over an impedance plane," The Journal of the Acoustical Society of America **116**(6), 3304–3311.

Ogilvy, J. A. (**1991**). *Theory of wave scattering from random rough surfaces* (Adam Hilger, London), 277 pages.

Ol'shevskii, V. (**1978**). *Statistical methods in sonar* (Consultants Bureau, New York, NY, USA), 242 pages.

Pearson, D. B. (**2001**). *Encyclopedia of Mathematics*, Chap. Sturm–Liouville theory (EMS Press, Berlin).

Polack, J.-D. (**1988**). "La transmission de l'énergie sonore dans les salles (*The transmission of sound energy in rooms*)," Ph.D. thesis, Université du Maine, Le Mans, France.

Polack, J.-D. (**1992**). "Modifying chambers to play billiards: the foundations of reverberation theory," Acta Acustica united with Acustica **76**(6), 256–272.

Ratilal, P., and Makris, N. C. (**2005**). "Mean and covariance of the forward field propagated through a stratified ocean waveguide with three-dimensional random inhomogeneities," The Journal of the Acoustical Society of America **118**(6), 3532–3559.

Schot, S. H. (**1992**). "Eighty years of Sommerfeld's radiation condition," Historia Mathematica **19**(4), 385–401.

Schroeder, M. R. (**1962**). "Frequency-correlation functions of frequency responses in rooms," The Journal of the Acoustical Society of America **34**(12), 1819–1823.

Weyl, H. (**1911**). "Ueber die asymptotische verteilung der eigenwerte (*On the asymptotic distribution of eigenvalues*)," Nachrichten von der Gesellschaft der Wissenschaften zu Göttingen, Mathematisch-Physikalische Klasse **1911**, 110–117.